INORGANIC CHEMISTRY
FRONTIERS

RESEARCH ARTICLE

Cite this: *Inorg. Chem. Front.*, 2021, **8**, 4634

Hydrogenation reactions catalyzed by HN($CH_2CH_2PR_2$)$_2$-ligated copper complexes†

Dewmi A. Ekanayake, Arundhoti Chakraborty, Jeanette A. Krause and Hairong Guan*

Received 20th June 2021,
Accepted 28th August 2021

DOI: 10.1039/d1qi00776a

rsc.li/frontiers-inorganic

HN($CH_2CH_2PR_2$)$_2$-ligated copper borohydride complexes, (^{R}PN^{H}P)Cu(BH_4) (R = ^{i}Pr, Cy, ^{t}Bu), which can be prepared from (^{R}PN^{H}P)CuBr and $NaBH_4$, are capable of catalyzing the hydrogenation of aldehydes in an alcoholic solvent. More active hydrogenation catalysts are (^{R}PN^{H}P)CuBr mixed with KO^{t}Bu, allowing various aldehydes and ketones to be efficiently reduced to alcohols except those bearing a nitro, *N*-unprotected pyrrole, pyridine, or an ester group, or those prone to aldol condensation (*e.g.*, 1-heptanal). Modifying the catalyst structure by replacing the NH group in (^{iPr}PN^{H}P)CuBr with an NMe group results in an inferior catalyst but preserves some catalytic activity. The hexanuclear copper hydride cluster, (^{iPr}PN^{H}P)$_3$$Cu_6H_6$, is also competent in catalyzing the hydrogenation of aldehydes such as benzaldehyde and *N*-methyl-2-pyrrolecarboxaldehyde, albeit accompanied by decomposition pathways. The catalytic performance can be enhanced through the addition of a strong base or ^{iPr}PN^{H}P. The three catalytic systems likely share the same catalytically active species, which is proposed to be a mononuclear copper hydride (^{R}PN^{H}P)CuH with the NH group bound to copper.

Introduction

Catalytic reduction of carbonyl compounds has been researched for decades owing to its importance in chemical synthesis, though in recent years efforts have been devoted more to the development of first row metal-based catalysts.[1] Among various reduction strategies, hydrogenation reactions are often preferred when the costs of the reductant and waste disposal outweigh the risks and capital costs for working with a flammable gas. One popular class of pro-ligands used to design catalysts specifically for carbonyl hydrogenation involves a diphosphine of the type HN($CH_2CH_2PR_2$)$_2$ (^{R}PN^{H}P for short),[2] which typically binds to metals through the [PNP] donor array. The presence of a metal-bound NH group is thought to play a crucial role in activating the C═O bond and stabilizing high-energy intermediates.[2,3] While the electronic configuration of the metal ion and the molecular geometry are undoubtedly important for catalysis, metal complexes bearing a (^{R}PN^{H}P)MH (M = Ru, Os, Ir, Re, Mo, Fe, Co, Mn) component[2] are almost universally successful in catalyzing the hydrogenation of C═O bonds with very few exceptions (*e.g.*, when M = Ni).[4]

Copper-based catalysts for carbonyl hydrogenation have been known since the late 1980s when Stryker's reagent, $(Ph_3P)_6Cu_6H_6$, was studied for the reduction of α,β-unsaturated aldehydes and ketones.[5] Depending on the hydrogen pressure, 2-cyclohexen-1-one is selectively converted to cyclohexanone (p_{H_2} = 65 psig) or cyclohexanol (p_{H_2} > 185 psig, over an extended period of time). Under the hydrogenation conditions, the catalyst degrades to black particles, which is avoidable through the addition of excess Ph_3P, leading to selective hydrogenation of the C═C–C═O moiety over an isolated C═C bond.[5b] Catalytic hydrogenation of simple ketones using well-defined copper hydrides such as $(Ph_3P)_6Cu_6H_6$, (κ^2-triphos)$_2$$Cu_2H_2$ (triphos = 1,1,1-tris(diphenylphosphinomethyl) ethane), and (dppp)$_4$$Cu_8H_8$ (dppp = 1,3-bis(diphenylphosphino)propane) proves to be unsuccessful unless the pro-ligand is also added (*e.g.*, $(Ph_3P)_6Cu_6H_6$ with 36 equiv. Me_2PPh; (κ^2-triphos)$_2$$Cu_2H_2$ with 1–1.5 equiv. triphos).[6] However, exactly how these added pro-ligands promote the reduction is not well understood. For the hydrogenation of CO_2 to formate,[7] the cationic copper hydride [(κ^3-triphos)$_2$$Cu_2H$]$^+$ alone is an efficient catalyst.[8] According to the proposed mechanism, 1,8-diazabicyclo[5.4.0]undec-7-ene (DBU), which is the base needed to drive the reaction, plays another role by breaking the Cu(μ-H)Cu core to yield [(κ^3-triphos)Cu(DBU)]$^+$ and the presumed active species (κ^3-triphos)CuH.[8,9] A very recent study by the Tanase group shows

Department of Chemistry, University of Cincinnati, P.O. Box 210172, Cincinnati, Ohio 45221-0172, USA. E-mail: hairong.guan@uc.edu; Tel: +1-513-556-6377

†Electronic supplementary information (ESI) available: NMR and IR spectra of the copper complexes, and X-ray crystallographic information. CCDC 2089300–2089302. For ESI and crystallographic data in CIF or other electronic format see DOI: 10.1039/d1qi00776a

that larger copper clusters, $[(\mu\text{-dpmppm})_3Cu_8H_6](PF_6)_2$ (dpmppm = $Ph_2PCH_2P(Ph)CH_2P(Ph)CH_2PPh_2$) and its CO_2 insertion product $[(\mu\text{-dpmppm})_2Cu_4(OCHO)_3]PF_6$, are also capable of catalyzing the hydrogenation of CO_2 to HCO_2^- in the presence of DBU.[10]

There are also a number of studies involving *in situ* generated but structurally ill-defined copper hydrides for catalytic hydrogenation of C=O bonds. In particular, copper-catalyzed asymmetric hydrogenation of ketones is often carried out using a chiral phosphine mixed with $Cu(OAc)_2$, $CuCl_2$, or $Cu(NO_3)(PAr_3)_2$.[11] These catalytic systems typically require a large excess of strong base (6–25 equiv. per copper) and, in some cases,[11a–d] additional PAr_3 to stabilize the catalysts. A similar catalytic protocol has been applied to chemoselective hydrogenation of aldehydes.[12] Hydrogenation of CO_2 to formate in the presence of DBU or a secondary amine can also be catalyzed by $Cu(OAc)_2$,[13] $Cu(OAc)_2$-DMAP (DMAP = 4-dimethylaminopyridine),[14] or (dtbpf)CuI (dtbpf = 1,1′-bis(di-*tert*-butylphosphino)ferrocene).[15] Considering that copper hydrides are usually air sensitive,[7,16] using a simple copper salt such as $Cu(OAc)_2$ to catalyze the hydrogenation reactions is synthetically more attractive; however, very limited mechanistic details can be gained from these studies.

This work fills several knowledge gaps concerning hydrogenation catalysis with copper. First, although $^{R}PN^{H}P$-ligated copper complexes have been known for a decade,[17] they have not been reported as hydrogenation catalysts until now. Our recent study shows that, unlike other metal systems, the putative "($^{R}PN^{H}P$)CuH" has the tendency to form clusters with only the phosphorus donors bound to copper (along with fully dissociated $^{R}PN^{H}P$, see Scheme 1).[18] This raises an interesting mechanistic question regarding the role that the NH group may or may not need to play during the hydrogenation process, which is addressed in this work. We have also previously observed the expansion of clusters from $(^{R}PN^{H}P)_2Cu_4H_4$ (R = ^{i}Pr, Cy) to $(^{R}PN^{H}P)_3Cu_6H_6$ and, in one case (R = ^{i}Pr), the release of $(^{R}PN^{H}P)_2Cu_4H_4$ when $(^{R}PN^{H}P)_3Cu_6H_6$ is treated with PhCHO.[18] Further mechanistic investigation presented herein paves the road for a better understanding of how the formation of copper hydride clusters impacts the overall hydrogenation reactions. Also studied here are the effects of base additives, which have been routinely used in conjunction with copper-based hydrogenation catalysts.

Results and discussion

($^{R}PN^{H}P$)Cu(BH_4) as hydrogenation catalysts

From the outset, we sought a more straightforward method of generating ($^{R}PN^{H}P$)CuH *in situ* to catalyze the hydrogenation of C=O bonds. Metal borohydride complexes $L_nM(BH_4)$ can be metal hydride complexes L_nMH in disguise, and if needed, a base can be added to assist the removal of BH_3.[19] For systems in which the hydride species are thermally unstable, it is advantageous to employ the more stable borohydride derivatives as hydrogenation catalysts. Successful examples known to date have been primarily focused on group 8 metal complexes such as *trans*-RuH(BH_4)(P-P)(1,2-diamine) (P-P = a diphosphine or diphosphinite),[20] ($^{R}PN^{H}P$)RuH(CO)(BH_4),[21] ($^{R}PN^{H}P$)FeHL(BH_4) (L = CO or CNR′),[22] and ($^{iPr}PN^{Me}P$)FeH(CNR′)(BH_4) ($^{iPr}PN^{Me}P$ = $MeN(CH_2CH_2P^{i}Pr_2)_2$).[23] For copper-based systems, borohydride complexes are known in the literature,[24] although they have not yet been described in hydrogenation studies.

The target copper borohydride complexes bearing a $^{R}PN^{H}P$ ligand were readily synthesized by treating ($^{R}PN^{H}P$)CuBr (**1a–c**) with excess $NaBH_4$ (eqn (1)). The isolated products, which are white solids, can be exposed to air for several hours without noticeable color or spectral change. Under an inert atmosphere, a solution sample of **2a** in C_6D_6 was shown to survive mild heating (50 °C) for at least 2 h but, after 24 h, yield a very small amount of black particles. Nevertheless, its thermal stability is significantly higher than that of the copper hydride complex, ($^{iPr}PN^{H}P)_3Cu_6H_6$ (**3a**), which starts to decompose in hours even if kept at room temperature.

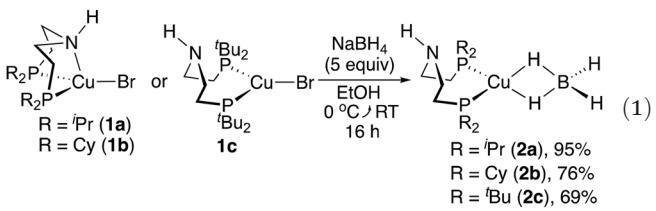

(1)

2a–c were characterized by NMR and IR spectroscopy as well as elemental analysis. For samples dissolved in C_6D_6, the BH_4 proton resonances cannot be definitively located due to broadening and overlap with the resonances of the phosphorus substituents (*i.e.*, the R groups). The ^{11}B NMR spectra, on the other hand, show a distinctive boron resonance near −30 ppm (Table 1), which is resolved as a quintet for **2a** and

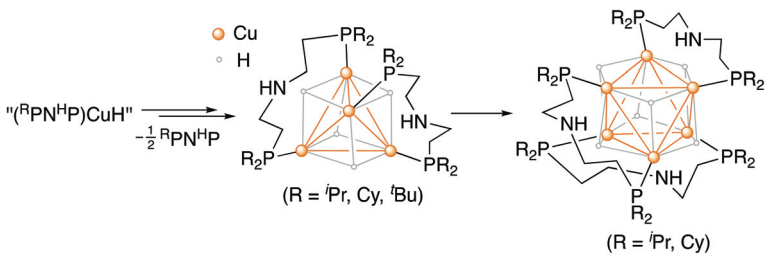

Scheme 1 Aggregation of the putative "($^{R}PN^{H}P$)CuH".

Table 1 Selected NMR and IR data of **2a–c** and the corresponding pro-ligands

Compound	δ_B (ppm)	ν_{N-H} (cm^{-1})	$\nu_{B-H\ terminal}$ (cm^{-1})	$\nu_{B-H\ bridging}$ (cm^{-1})
($^{iPr}PN^HP$)Cu(BH_4) (**2a**)	−29.0 (quint)	3305	2355	2020
$^{iPr}PN^HP$		3285		
($^{Cy}PN^HP$)Cu(BH_4) (**2b**)	−29.8 (br)	3304	2349, 2338	2022
$^{Cy}PN^HP$		3288		
($^{tBu}PN^HP$)Cu(BH_4) (**2c**)	−27.6 (quint)	3299	2353	2058
$^{tBu}PN^HP$		3288		

2c. At least one $B–H_{terminal}$ and one $B–H_{bridging}$ stretching bands can be identified from each IR spectrum (of a solid sample). The frequencies are very similar to those reported for other phosphine-ligated copper borohydride complexes.[24] It is interesting to note that the N–H stretching vibration of each copper complex is blue-shifted relative to $^RPN^HP$. This result argues against nitrogen coordination, which usually causes a decrease in the N–H stretching frequency.[25] The reason for the blue-shift is unclear; the N–H bond contraction can be a result of short-range repulsive forces or electric field effects exerted by the neighboring molecule.[26]

The solid-state structures of **2a** (Fig. 1) and **2c** (see Fig. S36 in the ESI†) studied by X-ray crystallography establish the κ^2-coordination mode for the BH_4 ligand and the absence of nitrogen coordination. Given that $^{iPr}PN^HP$ in **1a** serves as a tridentate ligand,[17] the Cu–H bond must be stronger than an N → Cu bond. Additional driving forces for nitrogen dissociation might come from intermolecular electrostatic interactions between the NH and BH_2 groups, as revealed by the crystal packing ($NH^{\delta+}\cdots^{\delta-}$ HB distance: 2.32–2.98 Å).

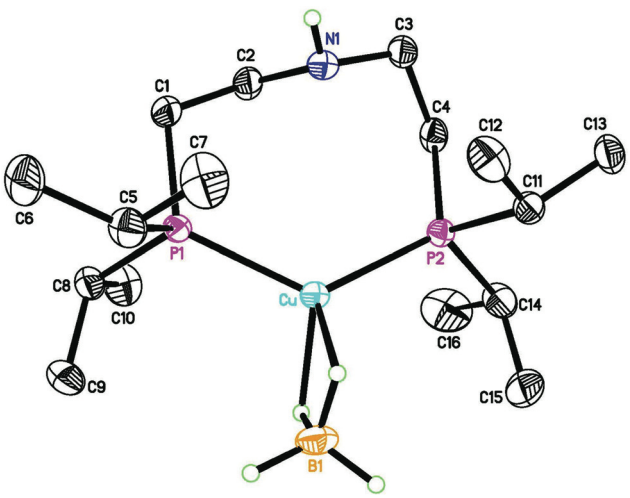

Fig. 1 ORTEP drawing of ($^{iPr}PN^HP$)Cu(BH_4) (**2a**) at the 50% probability level (hydrogen atoms bound to nitrogen and boron were located directly from the difference map and their coordinates were refined; all other hydrogen atoms were calculated and treated with a riding model and omitted here for clarity). Selected distances (Å) and angles (°): Cu–P(1) 2.2605(5), Cu–P(2) 2.2525(5), Cu–B(1) 2.2232(24), Cu···N(1) 3.4471(18); P(1)–Cu–P(2) 127.95(2), B(1)–Cu–P(1) 112.11(7), B(1)–Cu–P(2) 119.52(7), H–Cu–H 65.4(11).

Catalytic activities of **2a–c** (2 mol% loading) for hydrogenation reactions were evaluated at room temperature under 50 psig (or 4.4 bar) H_2 pressure for 24 h. As summarized in Table 2, in THF, all three copper borohydride complexes reduce approximately a stoichiometric amount of PhCHO (entries 1–3). The reduction becomes catalytic when the reaction is carried out in an alcoholic solvent (entries 4–8). Of the three catalysts tested in ^{i}PrOH, **2b** is the most active one, resulting in a 99% conversion of PhCHO to $PhCH_2OH$ (entry 7). Under an argon atmosphere using **2a** as the catalyst, 5% of PhCHO is reduced to $PhCH_2OH$ (entry 9), implying that transfer hydrogenation might be operative but would be significantly slower than direct hydrogenation. The addition of KO^tBu in a catalytic amount makes the hydrogenation of PhCHO in THF viable, although the Tishchenko product,[27] $PhCO_2CH_2Ph$, is also produced (entry 10). Reduction of $4\text{-}CF_3C_6H_4CHO$, which contains a more reactive carbonyl group, can be performed in both THF (entry 11) and ^{i}PrOH (entry 12). Again, the alcoholic solvent renders the hydrogen-

Table 2 Hydrogenation of aldehydes catalyzed by **2a–c** [a]

$$ArCHO + H_2\ (50\ psig) \xrightarrow[RT,\ 24\ h]{2\ mol\%\ [Cu]} ArCH_2OH$$

Entry	ArCHO	[Cu]	Solvent	KO^tBu (mol%)	Conversion[b] (%)
1	PhCHO	**2a**	THF	0	1
2	PhCHO	**2b**	THF	0	2
3	PhCHO	**2c**	THF	0	2
4	PhCHO	**2a**	MeOH	0	46
5	PhCHO	**2a**	EtOH	0	51
6	PhCHO	**2a**	^{i}PrOH	0	64
7	PhCHO	**2b**	^{i}PrOH	0	99
8	PhCHO	**2c**	^{i}PrOH	0	6
9[c]	PhCHO	**2a**	^{i}PrOH	0	5
10	PhCHO	**2a**	THF	2.4	48(19)[d]
11	$4\text{-}CF_3C_6H_4CHO$	**2a**	THF	0	7
12	$4\text{-}CF_3C_6H_4CHO$	**2a**	^{i}PrOH	0	>99
13	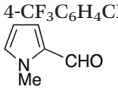	**2a**	^{i}PrOH	0	0
14	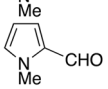	**2a**	^{i}PrOH	2	1

[a] Standard conditions: ArCHO (1.0 mmol) and copper catalyst (0.020 mmol) in THF or an alcoholic solvent (3 mL), under H_2 (50 psig), at room temperature (23 °C), stirred for 24 h. [b] Determined by ^{1}H NMR spectroscopy. [c] The reaction was carried out under argon (1 bar) instead of H_2. [d] The number in the parenthesis is the conversion of PhCHO to $PhCO_2CH_2Ph$.

ation process more efficient. We have previously reported that *N*-methyl-2-pyrrolecarboxaldehyde undergoes insertion into the Cu–H bond of ($^{i\text{Pr}}$PN$^{\text{H}}$P)$_3$Cu$_6$H$_6$ (**3a**).[18] To our disappointment, this specific aldehyde resists hydrogenation under the catalytic conditions that are effective for PhCHO and 4-$CF_3C_6H_4$CHO (entry 13). The addition of KO^{t}Bu does not appear to improve the catalytic reaction (entry 14).

NMR studies of **2a** in CD_3OD shed some light on why alcoholic solvents favor the hydrogenation process. The copper borohydride complex proves to be stable in CD_3OD for at least several days, at which point a small amount of HD (δ_H = 4.52 ppm, triplet, J_{H-D} = 42.8 Hz) can be detected. The ^{11}B NMR spectrum shows a quintet at −30.9 ppm for the BH_4 resonance along with a singlet at 3.0 ppm consistent with $[B(OCD_3)_4]^-$.[28] Thus it is tempting to propose that iterative protonation of the B–H bonds in **2a** by an alcohol will eventually unmask ($^{i\text{Pr}}$PN$^{\text{H}}$P)CuH to initiate carbonyl reduction. However, these protonation steps are considerably slower than the overall hydrogenation reaction. The BH_4 resonance of **2a** in the ^{1}H NMR spectrum is observed as a relatively sharp quartet at 0.71 ppm (J_{H-B} = 81 Hz), suggesting increased symmetry around the quadrupolar nucleus ^{11}B. CD_3OD is likely to cause the departure of BH_4^- from **2a** to form a solvent-separated ion-pair, which in turn reduces aldehydes in a similar way as $NaBH_4$. If all B–H bonds are available for the reduction, only the experiments with a conversion of >8% (entries 4–7, 10, and 12) can be confidently interpreted as copper-catalyzed hydrogenation reactions. Under such a scenario, dihydrogen activation by copper is required and presumably made possible *via* hydrogenolysis of a copper alkoxide intermediate.[29]

To further understand the reaction mechanism, hydrogenation of PhCHO in ^{i}PrOH catalyzed by **2b** was performed with D_2 in place of H_2. For the purpose of deriving the kinetic isotope effect (KIE), reaction conditions were chosen so that only 20–40% of PhCHO was reduced. As illustrated in Scheme 2, under D_2, 15% of PhCHO is reduced to PhCHDOH and 8% of PhCHO is converted to $PhCH_2OH$. The latter is likely a result of stoichiometric reduction of PhCHO by **2b**. Under the same conditions but with H_2, 37% of PhCHO is reduced to $PhCH_2OH$, giving a KIE value of 1.9 for the hydrogenation process. This result suggests that dihydrogen activation is involved in the turnover-limiting step.

($^{\text{R}}$PN$^{\text{H}}$P)CuBr mixed with KO^{t}Bu as hydrogenation catalysts

The limited catalytic activities observed for ($^{\text{R}}$PN$^{\text{H}}$P)Cu(BH_4) prompted us to resort to the conditions under which clusters ($^{\text{R}}$PN$^{\text{H}}$P)$_n$Cu$_{2n}$H$_{2n}$ (n = 2, 3) are produced (*i.e.*, mixing ($^{\text{R}}$PN$^{\text{H}}$P) CuBr with KO^{t}Bu under H_2).[18] We surmised that, in the presence of a carbonyl substrate, the initially formed ($^{\text{R}}$PN$^{\text{H}}$P)CuH might enter the catalytic cycle for the hydrogenation rather than engage in the aggregation illustrated in Scheme 1. Optimizations focusing on room-temperature hydrogenation of PhCHO catalyzed by **1a** and KO^{t}Bu (added in slight excess) show that, in THF, a catalyst loading of 2 mol% and a H_2 pressure of 50 psig are sufficient for the reaction to occur. After 24 h, 98% of PhCHO is reduced to $PhCH_2OH$ while the remaining aldehyde is converted to $PhCO_2CH_2Ph$ (Table 3, entry 1). Changing the catalyst to the cyclohexyl derivative (**1b**) results in a cleaner reduction of PhCHO and shortens the reaction time to 6 h (entry 2). In contrast, using the *tert*-butyl derivative (**1c**) makes the hydrogenation process more sluggish and yields more $PhCO_2CH_2Ph$ (entry 3). The hydrogenation reaction can also be performed in toluene, dioxane, and Et_2O, though less efficiently (entries 4–6). Lowering the H_2 pressure to 30 psig (entry 7) or raising the temperature to 50 °C (entry 8) leads to a precipitous drop in the conversion of PhCHO to $PhCH_2OH$. The $^{\text{R}}$PN$^{\text{H}}$P ligand is clearly needed; without it, the Tishchenko reaction converting PhCHO to $PhCO_2CH_2Ph$ becomes the more dominant pathway (entry 9). Because KO^{t}Bu[30] and metal alkoxides[27] are known to catalyze the Tishchenko reaction, their steady-state concentrations should be kept low to minimize the ester formation. Consistent with this hypothesis, reducing the amount of KO^{t}Bu from 2.4 to 2.0 mol% suppresses the formation of $PhCO_2CH_2Ph$ completely (entry 10), whereas adding more KO^{t}Bu increases the percentage of PhCHO being converted to the ester (entry 11). It should be noted that, in the absence of KO^{t}Bu, **1a** alone is not a hydrogenation catalyst (entry 12). Finally, using the optimized **1a**-to-KO^{t}Bu ratio (1 : 1), PhCHO is almost fully reduced to $PhCH_2OH$ in 3 h under 65 psig H_2 pressure (entry 13) or in 1 h under 80 psig H_2 pressure (entry 14).

The substrate scope of the copper-catalyzed hydrogenation reactions was explored by employing **1a**-KO^{t}Bu as the catalyst (2 mol% loading). The results for aldehydes are summarized in Table 4. Under the conditions optimized for PhCHO (p_{H2} = 50 psig, room temperature, 24 h), benzaldehyde derivatives bearing an electron-donating or a weakly electron-withdrawing group at the *para* position are hydrogenated nearly quantitatively to yield the corresponding alcohols. In our recent study of the reactions between {2,6-(^{i}Pr$_2$PO)$_2$C$_6$H$_3$}NiH and aldehydes,[31] 4-$CF_3C_6H_4$CHO was shown to perform consecutive insertions more readily than PhCHO which, following a β-hydride elimination step, gave the Tishchenko product. In line with this finding, hydrogenation of 4-$CF_3C_6H_4$CHO catalyzed by **1a**-KO^{t}Bu is plagued by the competing ester-forming process. A selectivity of 95% for 4-$CF_3C_6H_4CH_2OH$ can be achieved when the H_2 pressure is increased to 80 psig and the reaction mixture is diluted by twofold. Hydrogenation of 4-$NO_2C_6H_4$CHO is incomplete after 24 h even under 80 psig H_2 pressure (44% conversion), likely due to oxidation of the copper hydride intermediate by the nitro group. 2-Naphthaldehyde, 2-$CH_3C_6H_4$CHO, and 2-FC_6H_4CHO react more slowly than PhCHO and their *para*-isomers, thus

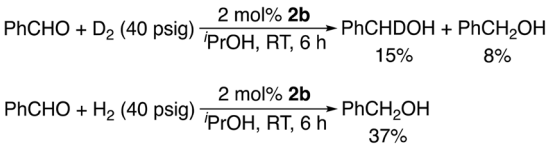

Scheme 2 Kinetic isotope effect for the hydrogenation of PhCHO.

Table 3 Hydrogenation of PhCHO catalyzed by **1a–c** along with KO^{t}Bu[a]

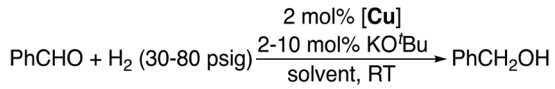

Entry	[Cu]	KO^{t}Bu (mol%)	Solvent	p_{H_2} (psig)	Time (h)	Conversion[b,c] (%)
1	**1a**	2.4	THF	50	24	98(2)
2	**1b**	2.4	THF	50	6	>99(0)
3	**1c**	2.4	THF	50	24	21(10)
4	**1a**	2.4	Toluene	50	24	90(3)
5	**1a**	2.4	Dioxane	50	24	85(2)
6	**1a**	2.4	Et_2O	50	24	15(2)
7	**1a**	2.4	THF	30	24	8(19)
8[d]	**1a**	2.4	THF	50	24	6(10)
9	CuBr	2.4	THF	50	6	5(21)
10	**1a**	2.0	THF	50	24	>99(0)
11	**1a**	10	THF	50	24	66(28)
12	**1a**	0	THF	50	6	0(0)
13	**1a**	2.0	THF	65	3	99(0)
14	**1a**	2.0	THF	80	1	98(0)

[a] Standard conditions: PhCHO (1.0 mmol), copper complex (0.020 mmol), and KO^{t}Bu in a solvent (3 mL), under H_2, stirred at room temperature (23 °C). [b] Determined by ^{1}H NMR spectroscopy. [c] Numbers in the parentheses are the conversions of PhCHO to $PhCO_2CH_2Ph$. [d] Stirred at 50 °C.

Table 4 Hydrogenation of various aldehydes catalyzed by **1a** along with KO^{t}Bu[a]

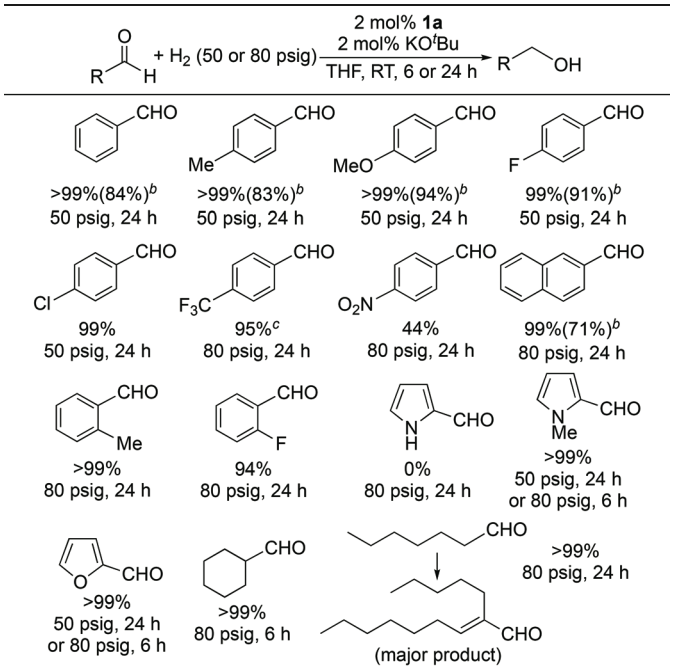

[a] Standard conditions: RCHO (1.0 mmol), **1a** (0.020 mmol), and KO^{t}Bu (0.020 mmol) in THF (3 mL), under H_2 (50 or 80 psig), stirred at room temperature (23 °C); conversions were determined by ^{1}H NMR spectroscopy. [b] Numbers in the parentheses are isolated yields. [c] The volume of THF was increased to 6 mL; 5% of RCHO was converted to RCO_2CH_2R.

Table 5 Hydrogenation of various ketones catalyzed by **1a** along with KO^{t}Bu[a]

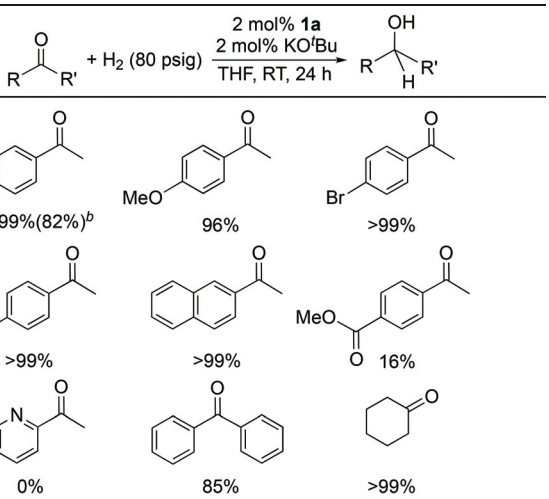

[a] Standard conditions: RCOR′ (1.0 mmol), **1a** (0.020 mmol), and KO^{t}Bu (0.020 mmol) in THF (3 mL), under H_2 (80 psig), stirred at room temperature (23 °C); conversions were determined by ^{1}H NMR spectroscopy. [b] The number in the parenthesis is the isolated yield.

requiring a slightly higher H_2 pressure (80 psig). Pyrrole-2-carboxaldehyde is not a viable substrate for the catalytic system. The NH moiety must prevent dihydrogen activation by strongly interacting with copper, which is indirectly confirmed by successful hydrogenation of *N*-methyl-2-pyrrolecarboxaldehyde and furfural. Hydrogenation of aliphatic aldehydes is feasible, as successfully demonstrated with cyclohexanecarboxaldehyde. 1-Heptanal, on the other hand, mainly participates in aldol condensation reaction, forming (*E*)-2-pentyl-2-nonenal[32] as the major product.

Hydrogenation of ketones catalyzed by **1a**-KO^{t}Bu (2 mol% loading) was performed under 80 psig H_2 pressure. As shown in Table 5, a quantitative conversion of acetophenone to 1-phenylethanol can be accomplished in 24 h. Under the same conditions, acetophenone derivatives substituted by a methoxy,

bromo, or trifluoromethyl group at the *para* position or fused by a benzene ring (*e.g.*, 2-acetylnaphthalene) are hydrogenated smoothly to the corresponding alcohols. Hydrogenation of methyl 4-acetylbenzoate occurs selectively to the ketone functionality but with a surprisingly low conversion of 16%. A more problematic substrate is 2-acetylpyridine, which may deactivate the catalyst through nitrogen coordination. As representative examples for diaryl ketones and aliphatic ketones, benzophenone and cyclohexanone are reduced to diphenylmethanol and cyclohexanol, respectively, without any issues.

Given that aldehydes can be hydrogenated under a lower H_2 pressure than that for ketones (50 *vs.* 80 psig), an attempt was made to selectively reduce the aldehyde functionality of 4-acetylbenzaldehyde using the conditions optimized for benzaldehyde (Table 3, entry 10). Unfortunately, the reaction did not yield any alcohol product; instead, a highly insoluble material was obtained upon mixing the substrate with the catalyst. It is possible that 4-acetylbenzaldehyde oligomerized or polymerized *via* an iterative aldol reaction.

To probe the selectivity in the hydrogenation of α,β-unsaturated aldehydes and ketones, 2-cyclohexen-1-one, 4-phenyl-3-buten-2-one, and cinnamaldehyde were treated with 2 mol% **1a**-KO^{t}Bu (in THF) under 80 psig H_2 pressure. For reasons unclear to us, the two ketone substrates gave rise to a complicated mixture that was difficult to analyze.[33] In contrast, hydrogenation of cinnamaldehyde formed cinnamyl alcohol only, albeit with a low conversion (eqn (2)). The same chemoselectivity (C=O over C=C bond) has been observed in two other copper-based catalytic systems: (1) $(Ph_3P)_6Cu_6H_6$ (5 mol% Cu), Me_2PPh (6 equiv./Cu), ^{t}BuOH (40 equiv./Cu), in C_6H_6, 55 psig H_2, RT;[6a] (2) $Cu(NO_3)(PPh_3)_2$-$Ph_2P(CH_2)_4PPh_2$ (0.2 mol%), NaOH (10 equiv./Cu), in EtOH, 710 psig H_2, 50 °C.[12]

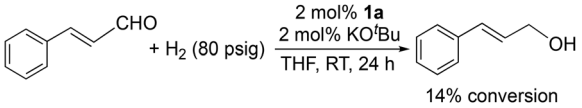

(2)

The aforementioned result indicates that the C=C bond in cinnamyl alcohol resists hydrogenation, which was confirmed separately by using pure cinnamyl alcohol as the substrate. Under the same conditions outlined in eqn (2), styrene, *trans*-β-methylstyrene, *trans*-stilbene, phenylacetylene, and 1-phenyl-1-propyne are completely unreactive (Scheme 3). Diphenylacetylene, however, shows some reactivity, giving *cis*-stilbene (4%) and *trans*-stilbene (5%) as determined by GC-MS and NMR.

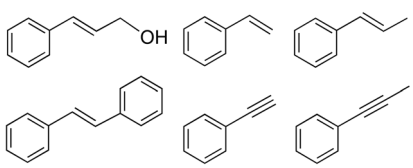

Scheme 3 Substrates resistant to hydrogenation.

$(^{iPr}PN^HP)_3Cu_6H_6$ as a hydrogenation catalyst

Without a reducible substrate, the reaction of **1a** with KO^{t}Bu under H_2 (Scheme 4) would generate $(^{iPr}PN^HP)_3Cu_6H_6$ (**3a**) along with $^{iPr}PN^HP$.[18] A smaller aggregate $(^{iPr}PN^HP)_2Cu_4H_4$ is also observable as the transient intermediate. The hexanuclear cluster can alternatively be prepared from $^{iPr}PN^HP$, CuBr, and KO^{t}Bu using the ligand-to-copper ratio suggested by the formula (1 : 2). Regardless of the routes used, the rates at which these clusters are formed (requiring 30–60 min) are comparable to the catalytic turnover frequencies (2–8 h^{-1}), suggesting that the cluster formation could be kinetically relevant for the hydrogenation process.

To further understand the catalytic roles that the hydride clusters might play, pure **3a** was employed as a hydrogenation catalyst. Because each molecule of **3a** contains six copper atoms, the catalyst loading was reduced to 0.34 mol% so that the total copper loading remained at 2 mol%. Hydrogenation of PhCHO (1 mmol in 3 mL of THF), as demonstrated in eqn (3), proves to be very slow, providing an essentially stoichiometric amount of $PhCH_2OH$. Interestingly, adding a catalytic amount of KO^{t}Bu accelerates the hydrogenation of PhCHO to $PhCH_2OH$. As expected, the presence of KO^{t}Bu also diverts 16% of PhCHO to $PhCO_2CH_2Ph$.

$$\begin{aligned}&\mathrm{PhCHO} + \mathrm{H_2}\,(80\,psig) \xrightarrow[\mathrm{THF,\,RT,\,3\,h}]{0.34\,\mathrm{mol\%}\ \mathbf{3a}} \mathrm{PhCH_2OH}\\ &\text{without KO}^t\text{Bu}: 2\%\ \text{to PhCH}_2\text{OH}\\ &\text{with 2 mol\% KO}^t\text{Bu}: 84\%\ \text{to PhCH}_2\text{OH}\end{aligned} \tag{3}$$

Compared to PhCHO, *N*-methyl-2-pyrrolecarboxaldehyde is less prone to forming the Tishchenko product. Its hydrogenation catalyzed by **3a** produces *N*-methyl-2-(hydroxymethyl) pyrrole exclusively, even when KO^{t}Bu is added (Table 6). Under the catalytic conditions that **1a**-KO^{t}Bu would reduce this aldehyde fully to the alcohol, **3a** is catalytically active but results in an incomplete reaction (entry 1). Similar to the outcomes shown in eqn (3), the addition of KO^{t}Bu or a related strong base such as LiO^{t}Bu and $NaN(SiMe_3)_2$ speeds up the hydrogenation process (entries 2–5). Screening of weak bases reveals that Et_3N increases the hydrogenation rate slightly (entry 6), whereas *N*,*N*-diisopropylethylamine and 2,6-lutidine slow down the reaction (entries 7 and 8). Phosphine oxides are known to stabilize Cu(I) and Cu(II) species,[34] and ^{t}BuOH is sometimes added to stabilize Cu(I) alkoxide intermediates (through alkoxide exchange to form the more stable

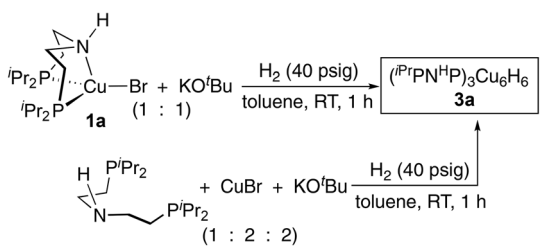

Scheme 4 Synthetic routes to the copper hydride cluster **3a**.

Table 6 Hydrogenation of *N*-methyl-2-pyrrolecarboxaldehyde catalyzed by **3a** [a]

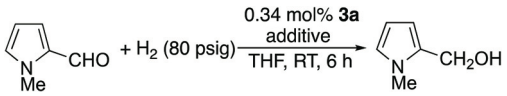

Entry	Additive	Conversion[b] (%)
1	None	63
2	KO^{t}Bu (2 mol%)	94
3	KO^{t}Bu (4 mol%)	95
4	LiO^{t}Bu (2 mol%)	91
5	NaN(SiMe$_3$)$_2$ (2 mol%)	96
6	Et$_3$N (2 mol%)	76
7	*N*,*N*-Diisopropylethylamine (2 mol%)	34
8	2,6-Lutidine (2 mol%)	41
9	Ph$_3$P=O (2 mol%)	61
10	^{t}BuOH (2 mol%)	59
11	^{iPr}PN^{H}P (1 mol%)	99

[a] Standard conditions: *N*-Methyl-2-pyrrolecarboxaldehyde (1.0 mmol), **3a** (0.0034 mmol, 2 mol% Cu), and an additive in THF (3 mL), under H_2 (80 psig), stirred at room temperature (23 °C). [b] Determined by ^{1}H NMR spectroscopy.

L_nCuO^tBu).[6a] Our results show that neither additive has any effect on the hydrogenation reaction (entries 9 and 10).

It is worth noting again that **3a** and the smaller aggregate (^{iPr}PN^{H}P)$_2$Cu$_4$H$_4$ have a ligand-to-copper ratio of 1 : 2 (Scheme 1). If the integrality of these clusters were maintained during the hydrogenation reaction, adding ^{iPr}PN^{H}P to the catalytic mixture could potentially interfere with the approach of the substrate and H_2 to copper. However, if the clusters needed to be broken down into (^{iPr}PN^{H}P)$_n$Cu$_n$H$_n$ (n = 1–3)[35] for the hydrogenation reaction to occur, added ^{iPr}PN^{H}P could be beneficial because in theory 50% of the CuH moieties would be unsupported and decompose to Cu(0) and H_2.[36] Consistent with the latter, adding 1 mol% ^{iPr}PN^{H}P leads to a marked improvement of the hydrogenation reaction (entry 11).

The NH effect

Hydrogenation catalysts bearing a (^{R}PN^{H}P)MH component often operate *via* a metal–ligand bifunctional mechanism in which the NH functionality activates the carbonyl substrates, stabilizes the intermediates following hydride transfer, and participates in dihydrogen activation, all enabled by the N–H···O hydrogen-bonding interactions (HBIs).[3] When the NH group is alkylated, these benefits disappear and the hydride becomes sterically less accessible, leading to inactive catalysts. The presence of an H–N–M–H unit, however, does not necessarily mean that the NH group is always involved in the hydrogenation mechanism. The H–N–M–H dihedral angle can be too wide (*e.g.*, 60° or higher) to participate in N–H···O HBIs that are conformationally restricted by the metal.[37] Furthermore, in some catalytic systems (*e.g.*, iron-catalyzed hydrogenation of CO_2), the N–H···O HBIs can be unimportant.[23,38] Alkylating the NH group in these catalysts makes little difference on the catalytic performance, or even shows improvement, possibly due to increased thermal stability for the *N*-alkylated catalysts.[37] The copper system presented in this work is unique in the sense that the NH binding is not guaranteed, which depends on the nature of the X-type ligand on Cu(I). For instance, nitrogen coordination is absent in (^{R}PN^{H}P)Cu(BH$_4$), (^{R}PN^{H}P)$_2$Cu$_4$H$_4$, and (^{R}PN^{H}P)$_3$Cu$_6$H$_6$, but present in (^{R}PN^{H}P)CuBr unless the phosphorus substituents are sufficiently bulky (R = ^{t}Bu, see structure of **1c** in eqn (1)). If the catalytically active species lack nitrogen coordination, alkylating the NH group is expected to have a minimal impact on the catalytic activity.[39]

Guided by this analysis, we prepared the *N*-methylated copper complex, (^{iPr}PN^{Me}P)CuBr (**4a**), from ^{iPr}PN^{Me}P and CuBr in THF (eqn (4)) and studied its structure by X-ray crystallography. As illustrated in Fig. 2, **4a** is a four-coordinate metal complex with the NMe group bound to copper. The geometry about copper is best described as trigonal pyramidal based on the geometry index (τ_4)[40] value of 0.83. The Me–N–Cu–Br dihedral angle of 19.68° is comparable to the H–N–Cu–Br dihedral angle in **1a** (24.89° and 25.62° for two independent molecules).[17] If the hypothesized hydride species (^{iPr}PN^{H}P)$_n$Cu$_n$H$_n$ (n = 1–3), especially the mononuclear one, do contain the H–N–Cu–H bond connectivity, the dihedral angle is likely similar, although at this point it is unclear if such angle (~20°) remains reasonable for a metal–ligand bifunctional catalyst.

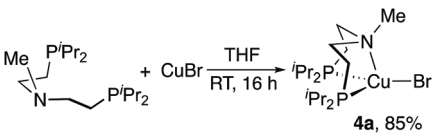

(4)

Catalytic performance of **4a**-KO^{t}Bu was investigated for the hydrogenation of PhCHO, *N*-methyl-2-pyrrolecarboxaldehyde, and PhCOCH$_3$ (Table 7). Under the conditions that **1a**-KO^{t}Bu would induce high conversions of the carbonyl substrates to the desired alcohols, **4a**-KO^{t}Bu displays very limited activity

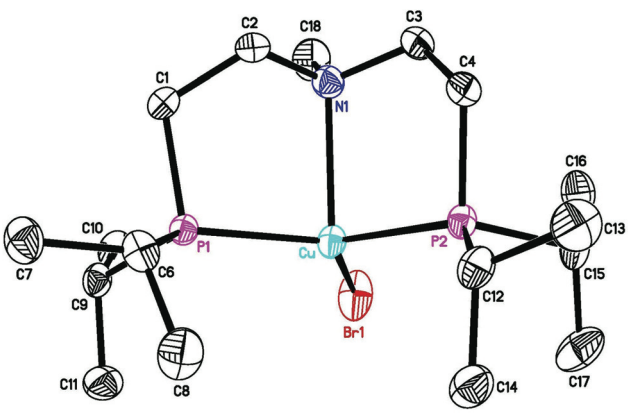

Fig. 2 ORTEP drawing of (^{iPr}PN^{Me}P)CuBr (**4a**) at the 50% probability level (all hydrogen atoms omitted for clarity). Selected distances (Å) and angles (°): Cu–P(1) 2.2400(6), Cu–P(2) 2.2363(6), Cu–Br(1) 2.4118(4), Cu–N(1) 2.3654(19); P(1)–Cu–P(2) 125.39(2), N(1)–Cu–P(1) 85.11(5), N(1)–Cu–P(2) 85.41(5), N(1)–Cu–Br(1) 108.87(5), P(1)–Cu–Br(1) 117.740(19), P(2)–Cu–Br(1) 116.228(19).

Table 7 Hydrogenation of C═O bonds catalyzed by **4a** along with KO^{t}Bu[a]

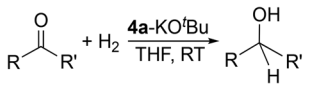

Entry	RCOR′	**4a** (mol%)	KO^{t}Bu (mol%)	p_{H_2} (psig)	Time (h)	Conversion[b,c] (%)
1	PhCHO	2	2.4	50	24	1(0.4)
2	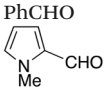	2	2	80	6	3
3	$PhCOCH_3$	2	2.4	80	24	0
4	PhCHO	10	12	50	24	54(43)
5	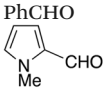	10	10	80	6	45

[a] Standard conditions: RCOR′ (1.0 mmol), **4a**, and KO^{t}Bu in THF (3 mL), under H_2 (50 or 80 psig), at room temperature (23 °C), stirred for 6 or 24 h. [b] Determined by ^{1}H NMR spectroscopy. [c] Numbers in the parentheses are the conversions of PhCHO to $PhCO_2CH_2Ph$.

(entries 1–3). For the reduction of the two aldehydes, increasing the catalyst loading by fivefold leads to a significant increase in alcohol formation and, in the case of PhCHO, also ester formation (entries 4 and 5). The amounts of alcohol products being formed suggest that these reactions are catalytic in copper and having an NH group is not absolutely required for the catalysts to be active. Nevertheless, the ^{R}PN^{H}P-ligated copper complex is substantially more reactive, suggesting that nitrogen coordination is most likely present in the catalytically active species.

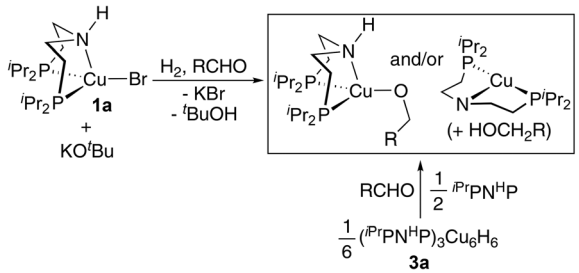

Scheme 5 Two catalytic systems converge to the same intermediate(s).

Mechanistic considerations

Among the three types of hydrogenation catalysts examined thus far, (^{R}PN^{H}P)CuBr mixed with KO^{t}Bu appears to be the most efficient one. It is possible that the copper bromide complexes react with KO^{t}Bu to yield (^{R}PN^{H}P)CuO^{t}Bu and/or T-shaped (^{R}PNP)Cu (with concomitant elimination of HO^{t}Bu),[41] which then activate H_2 to form copper hydrides. Indeed, the colorless solution of **1a** in C_6D_6 turns lemon yellow upon mixing with KO^{t}Bu (1 equiv.), indicating some reaction between these two compounds. ^{1}H and ^{31}P{^{1}H} NMR spectra show multiple products along with the unreacted **1a**. Unfortunately, efforts to isolate and characterize the products were thwarted by further decomposition during the workup.

Under the hydrogenation conditions, the colors of the reaction mixtures can provide useful, though not always definitive, information about the types of species present. When the hydrogenation reaction is catalyzed by the orange colored **3a** (Table 6, entry 1), the solution color is a brownish yellow. Adding $^{i\mathrm{Pr}}$PN^{H}P (Table 6, entry 11) changes the color first to golden yellow, then to lemon yellow as the reaction progresses. Based on these results, we propose that the hydride cluster reduces the carbonyl substrate and, in the presence of $^{i\mathrm{Pr}}$PN^{H}P, gradually forms the same copper species as those generated from the reaction catalyzed by **1a**-KO^{t}Bu (Scheme 5). Without the added $^{i\mathrm{Pr}}$PN^{H}P, at least 50% of **3a** decomposes to Cu(0) and other copper-containing products, which contributes to the darkening of the solution.

The reactivities of well-defined copper hydrides towards aldehydes and ketones have been investigated by several research groups. The seminal study by Caulton demonstrates that $[(p\text{-tolyl})_3P]_6Cu_6H_6$ reacts with HCHO to form HCO_2CH_3 catalytically, presumably *via* the intermediate $[(p\text{-tolyl})_3P]_nCuOCH_3$.[42] In Stryker's work, $(Ph_3P)_6Cu_6H_6$ transfers hydride to α,β-unsaturated ketones to yield copper enolate complexes but shows no reaction with cyclohexanone.[5b] This result should explain why $(Ph_3P)_6Cu_6H_6$ is a poor hydrogenation catalyst for simple ketones. In studying hydrosilylation mechanisms, Nikonov reported the insertion reaction of PhCHO with $(Ph_3P)_6Cu_6H_6$ which, after a day, gives $(Ph_3P)_nCuOCH_2Ph$ (65% NMR yield) as well as some metallic copper.[43] A recent study by Tran and Bullock focusing on $(NHC)_2Cu_2H_2$ (NHC = an N-heterocyclic carbene) confirms that the dinuclear hydride needs to dissociate to (NHC)CuH first, and the subsequent reaction with an aldehyde or a ketone produces a copper alkoxide complex.[44] As also demonstrated by Leyssens, Riant, and Sollogoub, a monomeric (NHC)CuH built inside a cyclodextrin reduces the carbonyl group of acetophenone and 4-phenyl-3-buten-2-one to yield an insertion product.[45] In our preliminary study, we have shown stoichiometric reduction of PhCHO, *N*-methyl-2-pyrrolecarboxaldehyde, and $PhCOCH_3$ by **3a** to give copper alkoxide species as the major products.[18] However, the complexity of the NMR spectra does not allow us to identify other products that are

potentially generated from these reactions (*e.g.*, (^{R}PNP)Cu and (^{R}PN^{H}P)CuOH resulting from hydrolysis of the alkoxide species).

For this work, we studied the reactivity of **3a** with additional substrates, especially the challenging ones for the catalytic reactions (Scheme 6). In a typical experiment, **3a** was mixed with a carbonyl substrate (10 equiv., or 1.7 equiv. on a per CuH basis) in C_6D_6 and the progress of the reaction was monitored by NMR spectroscopy. A successful insertion reaction with **3a** is usually signaled by a color change from orange to brownish yellow. Interestingly, adding 4-nitrobenzaldehyde to **3a** induces an immediate color change to dark green and then to black/brown in 30 min, consistent with a series of oxidation events by the nitro group. The reaction of pyrrole-2-carboxaldehyde with **3a** generates H_2 and **5a**,[46] which can be synthesized independently from **1a**, KO^{t}Bu, and pyrrole-2-carboxaldehyde (Scheme 7). This confirms our earlier hypothesis that the failure to hydrogenate this specific aldehyde is due to strong substrate binding. 1-Heptanal reacts with **3a** differently, giving (*E*)-2-pentyl-2-nonenal as the major organic product. The copper alkoxide species resulting from carbonyl insertion must act as a catalyst for the aldol condensation reaction. Methyl 4-acetylbenzoate and benzophenone undergo slow insertion, requiring days to fully consume **3a**. By comparison, the reaction of $PhCOCH_3$ with **3a** takes 2 h to complete. The reaction with 2-acetylpyridine is very complicated; in addition to the expected insertion product, several other unidentified by-products are also present. Overall, the outcomes of the stoichiometric reactions with **3a** more or less reflect how these carbonyl substrates are reduced catalytically by **1a**-KO^{t}Bu.[47]

The carbonyl insertion into the Cu–H bond of **3a** is an irreversible process, as established by no protio incorporation into the remaining PhCDO during the reaction of **3a** with 10 equiv. of PhCDO. Attempts to isolate the insertion products (*i.e.*, the copper alkoxide complexes) including the independent synthesis from **1a** and $NaOCH_2Ph$ have been fruitless. According to the study by Whitesides,[48] primary and secondary alkoxide complexes of Cu(I) can undergo facile thermal decomposition *via* radical intermediates. The added complication to the reaction of **3a** with a carbonyl substrate is that the insertion reaction is always accompanied by the decomposition of **3a**, in part due to the insufficient amount of the supporting ligand. The fact that KO^{t}Bu can enhance the catalytic reactivity of **3a** (eqn (3) and Table 6) encouraged us to study the stoichiometric reduction in the presence of added KO^{t}Bu. First, a control experiment confirms that KO^{t}Bu does not react with **3a**. Mixing *N*-methyl-2-pyrrolecarboxaldehyde with **3a** and KO^{t}Bu in a 10 : 1 : 1.2 ratio (in C_6D_6) generates the insertion product more cleanly than the reaction without KO^{t}Bu. In other words, the addition of KO^{t}Bu minimizes the degradation of **3a** during carbonyl insertion, possibly through the increase of negative charge on copper. Adding ^{iPr}PN^{H}P to the reaction of **3a** with *N*-methyl-2-pyrrolecarboxaldehyde can provide the similar benefit.

Taken together, we speculate that the catalytically active species is a mononuclear copper hydride (^{R}PN^{H}P)CuH with ^{R}PN^{H}P acting as a tridentate ligand. The hexanuclear clusters (^{R}PN^{H}P)$_3$Cu$_6$H$_6$ have an intense color (R = ^{i}Pr, bright orange; R = Cy, dark red), in contrast to the light yellow color typically observed for a productive hydrogenation reaction. We have also previously isolated tetranuclear clusters (^{R}PN^{H}P)$_2$Cu$_4$H$_4$ (R = Cy, ^{t}Bu) as off-white solids,[18] so the color alone cannot be used to rule out the involvement of aggregates. Furthermore, even species spectroscopically observable during the catalytic reaction may not be directly involved in the catalytic cycle. It should be pointed out, though, that the NH group does not coordinate to copper in (^{R}PN^{H}P)$_3$Cu$_6$H$_6$ and (^{R}PN^{H}P)$_2$Cu$_4$H$_4$. We have not yet had spectroscopic evidence for (^{R}PN^{H}P)$_n$Cu$_n$H$_n$ (n = 2, 3); however, based on reported structures of phosphine-ligated dinuclear[35a] and trinuclear[35c] copper hydrides (Scheme 8), the NH coordination is unlikely to be involved. Therefore, we would have anticipated similar catalytic activity exhibited by **1a**-KO^{t}Bu and **4a**-KO^{t}Bu. A significant NH effect, as observed experimentally, is expected for the mononuclear copper hydride (^{R}PN^{H}P)CuH where the NH coordination is most likely present.[49]

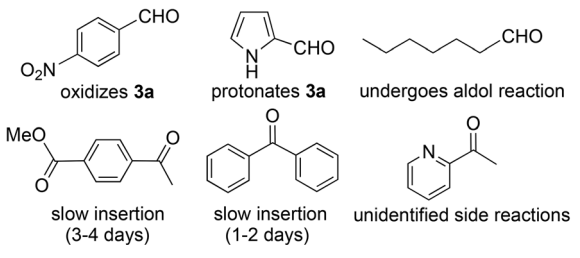

Scheme 6 Substrates that lead to low or no conversions to the alcohols.

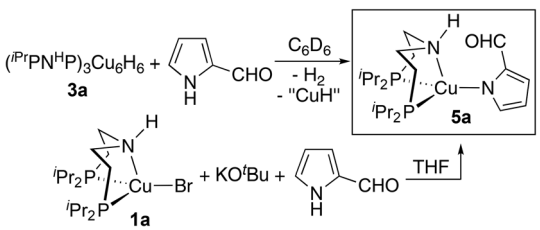

Scheme 7 Copper pyrrolide complex derived from pyrrole-2-carboxaldehyde.

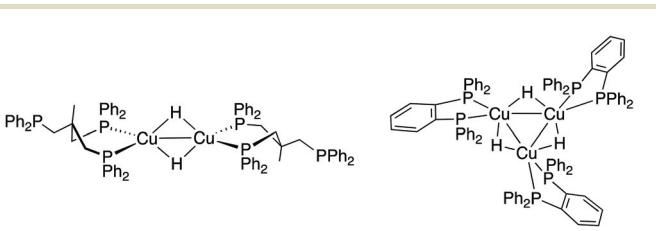

Scheme 8 Structures of phosphine-ligated dinuclear and trinuclear copper hydrides.

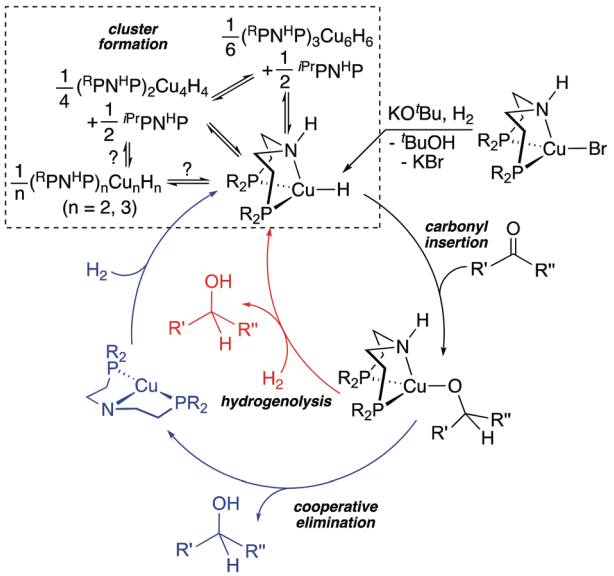

Scheme 9 Proposed hydrogenation mechanism.

Mechanistic pathways consistent with our experimental results are outlined in Scheme 9. Starting from (^{R}PN^{H}P)CuBr, its reaction with KO^{t}Bu under H_2 may generate the mononuclear copper hydride (^{R}PN^{H}P)CuH, which can aggregate to clusters under the following circumstances: (1) when the substrate is not added, (2) when the substrate is depleted at the end of hydrogenation, and (3) when the substrate reacts with (^{R}PN^{H}P)CuH slowly. The productive catalytic cycle begins with carbonyl insertion to form an alkoxide intermediate, which undergoes direct hydrogenolysis to regenerate (^{R}PN^{H}P)CuH while releasing the alcohol product. The hydrogenolysis step may require a prior dissociation of the NH group from copper. An alternative or perhaps parallel pathway relies on the NH hydrogen to eliminate the alcohol product from the alkoxide intermediate. The resulting T-shaped copper complex (^{R}PNP)Cu activates H_2 to close the catalytic cycle.[50] The observed H_2 pressure dependence (Table 3) and KIE (Scheme 2) imply that dihydrogen activation is the turnover-limiting step, at least for the hydrogenation of PhCHO. The turnover-limiting step could change to the insertion step when a less reactive carbonyl substrate is used. Alkylating the NH group shuts the cooperative elimination path from the alkoxide intermediate but still allows the hydrogenolysis to occur, which accounts for the observed catalytic activity with (^{R}PN^{Me}P)CuBr. The diminished activity could be due to the unfavorable steric effects on the insertion and hydrogenolysis steps and/or only one hydride-regeneration pathway being available. When the cluster (^{R}PN^{H}P)$_3$Cu$_6$H$_6$ is employed as the catalyst, it can dissociate to (^{R}PN^{H}P)CuH, thus entering the catalytic cycle. We cannot, however, rule out an insertion event on the cluster prior to cluster dissociation. Neither can we completely rule out the involvement of (^{R}PN^{H}P)$_n$Cu$_n$H$_n$ (n = 2, 3). In a simplistic view, (^{R}PN^{H}P)$_3$Cu$_6$H$_6$ should display 50% of the catalytic activity observed for (^{R}PN^{H}P)CuBr (on a per Cu basis), assuming that half of the copper sites are lost to the short-lived "CuH". In reality, other decomposition reactions also take place from (^{R}PN^{H}P)$_3$Cu$_6$H$_6$ and the extent of decomposition depends on the substrate used. For instance, the reduction of PhCHO with **3a** gives significantly more by-products than the reduction of *N*-methyl-2-pyrrolecarboxaldehyde, which can be used to rationalize the very low PhCHO-to-PhCH$_2$OH conversions shown in eqn (3) (without KO^{t}Bu). In any case, the addition of KO^{t}Bu or ^{R}PN^{H}P can minimize the degradation processes, leading to improved catalytic reactions.

Conclusions

In this work, we have shown catalytic hydrogenation of C=O bonds with three different types of copper complexes, all bearing a ^{R}PN^{H}P ligand: (^{R}PN^{H}P)Cu(BH$_4$) (R = ^{i}Pr, Cy), (^{R}PN^{H}P)CuBr-KO^{t}Bu (R = ^{i}Pr, Cy, ^{t}Bu), and (^{iPr}PN^{H}P)$_3$Cu$_6$H$_6$. The copper borohydride complexes exhibit the lowest catalytic activities. The reactions are best carried out in an alcoholic solvent, which assists the dissociation of BH_4^- from copper to initiate the reduction of aldehydes, first with BH_4^- and then with H_2. The copper bromide complexes, when combined with KO^{t}Bu, show the highest catalytic activities, allowing a variety of aldehydes and ketones to be hydrogenated to alcohols. Challenging substrates include 4-nitrobenzaldehyde, pyrrole-2-carboxaldehyde, 1-heptanal, and 2-acetylpyridine, and their intended hydrogenation reactions are impeded by other processes including oxidation or protonation of the hydride intermediates, aldol condensation, and strong binding to copper. Less polar double bonds such as those in styrene and phenylacetylene derivatives are resistant to the hydrogenation conditions. Replacing the NH group in (^{iPr}PN^{H}P)CuBr with an NMe group does not lead to a completely inactive catalyst, but the catalytic efficiency is significantly reduced. The hexanuclear copper hydride complex (^{iPr}PN^{H}P)$_3$Cu$_6$H$_6$ proves to be an active catalyst for aldehyde hydrogenation. It performs better than (^{iPr}PN^{H}P)Cu(BH$_4$) but worse than (^{iPr}PN^{H}P)CuBr-KO^{t}Bu for the hydrogenation of *N*-methyl-2-pyrrolecarboxaldehyde. The catalytic reactions can be improved through the addition of a strong base or ^{iPr}PN^{H}P.

Copper hydrides are inclined to aggregation to form clusters. For the ^{R}PN^{H}P-ligated system, they are known to yield the spectroscopically observable (^{R}PN^{H}P)$_2$Cu$_4$H$_4$ (R = ^{i}Pr, Cy, ^{t}Bu) and (^{R}PN^{H}P)$_3$Cu$_6$H$_6$ (R = ^{i}Pr, Cy), in which the central NH group does not coordinate to copper. The cluster-forming process is not slow enough to be completely irrelevant for the catalytic hydrogenation reactions. Though we favor a mononuclear copper hydride (^{R}PN^{H}P)CuH with the NH group bound to copper, the catalytically active species could also be a copper hydride cluster. We suspect that the aggregation process can become favorable when the substrates are less reactive towards (^{R}PN^{H}P)CuH.[51]

The effects of base additives have been examined for all three catalytic systems. In THF, with added KO^{t}Bu, the copper borohydride complexes show higher catalytic activities, likely

due to the removal of BH_3 to unmask the hydrides. The copper bromide complexes require 1 equiv. of KO^{t}Bu to fully activate the catalysts. An excess of KO^{t}Bu can be detrimental to the hydrogenation of aldehydes due to the base-catalyzed Tishchenko reaction. The hexanuclear copper hydride ($^{i\mathrm{Pr}}$PN$^{\mathrm{H}}$P)$_3$Cu$_6$H$_6$ displays an improved catalytic efficiency in the presence of KO^{t}Bu, which is shown to minimize the unproductive degradation of the cluster.

Experimental section

General considerations

All copper complexes described in this paper were prepared under an argon atmosphere using standard glovebox and Schlenk techniques. Benzene-d_6 (purchased from Cambridge Isotope Laboratories) was dried over sodium-benzophenone and distilled under an argon atmosphere. Methanol, ethanol, and 2-propanol (all purchased from Fisher Scientific) were dried over 4 Å molecular sieves and then deoxygenated by bubbling argon through them for one hour. All other dry and oxygen-free solvents used for synthesis and workup (CH_2Cl_2, *n*-pentane, THF, and toluene, all purchased from Fisher Scientific) were collected from an Innovative Technology solvent purification system. *N*-Methyl-2-pyrrolecarboxaldehyde and cyclohexanecarboxaldehyde were purchased from TCI America. Cyclohexanone and cinnamaldehyde were purchased from Fisher Scientific and Eastman Chemical, respectively. All other carbonyl substrates and D_2 (99.8% D) were purchased from Sigma-Aldrich. Prior to use, all liquid aldehydes were freshly distilled under argon and all liquid ketones were deoxygenated by bubbling argon through them for 30 min. ($^{i\mathrm{Pr}}$PN$^{\mathrm{H}}$P)CuBr (**1a**),[17] ($^{\mathrm{Cy}}$PN$^{\mathrm{H}}$P)CuBr (**1b**),[18] ($^{t\mathrm{Bu}}$PN$^{\mathrm{H}}$P)CuBr (**1c**),[18] $^{i\mathrm{Pr}}$PN$^{\mathrm{Me}}$P,[52] and ($^{i\mathrm{Pr}}$PN$^{\mathrm{H}}$P)$_3$Cu$_6$H$_6$ (**3a**)[18] were prepared according to literature procedures. Chemical shift values in ^{1}H and ^{13}C{^{1}H} NMR spectra were referenced internally to the residual solvent resonances. ^{31}P{^{1}H} and ^{11}B NMR spectra were referenced externally to 85% H_3PO_4 (0 ppm) and $BF_3{\cdot}OEt_2$ (0 ppm), respectively. Infrared spectra were recorded on a PerkinElmer Spectrum Two FT-IR spectrometer equipped with a smart orbit diamond attenuated total reflectance (ATR) accessory. High-resolution mass spectrometry data were acquired using a Thermo Scientific LTQ-FT hybrid mass spectrometer.

Synthesis of ($^{i\mathrm{Pr}}$PN$^{\mathrm{H}}$P)Cu(BH$_4$) (2a). A flame-dried Schlenk flask equipped with a stir bar was charged with **1a** (200 mg, 0.445 mmol) and $NaBH_4$ (84 mg, 2.22 mmol), and then chilled in an ice bath (0 °C). After slow addition of degassed EtOH (30 mL), the reaction mixture was gradually warmed to room temperature and stirred for 16 h. Removal of the volatiles under vacuum afforded a white solid, which was extracted with toluene (30 mL first and then 5 mL × 3) followed by filtration through Celite to give a colorless solution. Evaporation of the solvent under vacuum and then washing the residue with *n*-pentane (5 mL × 3) afforded the desired product as a white solid (164 mg, 95%). X-ray quality crystals were grown from a toluene/*n*-pentane solution. ^{1}H NMR (400 MHz, C_6D_6, δ): 2.63–2.41 (m, NCH_2, 4H), 1.83–1.69 (m, PCH(CH$_3$)$_2$, 4H), likely 1.56 (q, $J_{\mathrm{H-B}}$ = 82 Hz, BH_4, 4H), 1.26–1.13 (m, CH(CH_3)$_2$ + PCH_2, 16H), 1.00–0.83 (m, CH(CH_3)$_2$, 12H); the NH resonance was not located. ^{1}H NMR (400 MHz, CD_3OD, δ): 2.96–2.84 (m, NCH_2, 4H), 2.09–1.97 (m, PCH(CH$_3$)$_2$, 4H), 1.85–1.72 (m, PCH_2, 4H), 1.30–1.10 (m, CH(CH_3)$_2$, 24H), 0.71 (q, $J_{\mathrm{H-B}}$ = 81 Hz, BH_4, 4H); the NH resonance was not located. ^{13}C{^{1}H} NMR (101 MHz, C_6D_6, δ): 44.1 (t, $J_{\mathrm{C-P}}$ = 2.7 Hz, NCH_2), 24.0 (t, $J_{\mathrm{C-P}}$ = 9.3 Hz, CH(CH$_3$)$_2$), 19.7 (t, $J_{\mathrm{C-P}}$ = 5.7 Hz, PCH_2), 19.0 (t, $J_{\mathrm{C-P}}$ = 3.5 Hz, CH(CH_3)$_2$), 18.2 (t, $J_{\mathrm{C-P}}$ = 2.2 Hz, CH(CH_3)$_2$). ^{31}P{^{1}H} NMR (162 MHz, C_6D_6, δ): 2.6 (s). ^{11}B NMR (128 MHz, C_6D_6, δ): −29.0 (quint, $J_{\mathrm{B-H}}$ = 82.8 Hz). ^{11}B NMR (128 MHz, CD_3OD, δ): −30.9 (quint, $J_{\mathrm{B-H}}$ = 80.2 Hz). Selected ATR-IR data (solid, cm^{-1}): 3305 ($\nu_{\mathrm{N-H}}$), 2952, 2924, 2886, 2866, 2807, 2355 ($\nu_{\mathrm{B-H\ terminal}}$), 2232 ($\delta_{\mathrm{BH_2}}$ overtone), 2020 ($\nu_{\mathrm{B-H\ bridging}}$), 1944, 1458, 1362, 1127 ($\delta_{\mathrm{BH_2}}$). Anal. Calcd for $C_{16}H_{41}BCuNP_2$: C, 50.07; H, 10.77; N, 3.65. Found: C, 50.01; H, 10.86; N, 3.59.

Synthesis of ($^{\mathrm{Cy}}$PN$^{\mathrm{H}}$P)Cu(BH$_4$) (2b). This compound was obtained as a white solid in 76% yield (0.24 mmol scale reaction) following a procedure similar to that used for **2a**. ^{1}H NMR (400 MHz, C_6D_6, δ): 2.73–2.53 (m, NCH_2, 4H), 2.08–1.97 (m, 4H), 1.84–1.56 (m, 27H), 1.40–1.28 (m, 10H), 1.25–1.07 (m, CyH, 12H); the NH and BH resonances were not located. ^{13}C{^{1}H} NMR (101 MHz, C_6D_6, δ): 44.5 (s, NCH_2), 33.9 (t, $J_{\mathrm{C-P}}$ = 8.8 Hz, PCH), 29.0 (s, CyC), 28.8 (s, CyC), 27.5 (t, $J_{\mathrm{C-P}}$ = 5.9 Hz, CyC), 27.4 (t, $J_{\mathrm{C-P}}$ = 4.3 Hz, CyC), 26.6 (s, CyC), 20.1 (t, $J_{\mathrm{C-P}}$ = 5.9 Hz, PCH_2). ^{31}P{^{1}H} NMR (162 MHz, C_6D_6, δ): −6.1 (s). ^{11}B NMR (128 MHz, C_6D_6, δ): −29.8 (br). Selected ATR-IR data (solid, cm^{-1}): 3304 ($\nu_{\mathrm{N-H}}$), 2921, 2845, 2802, 2349 ($\nu_{\mathrm{B-H\ terminal}}$), 2338 ($\nu_{\mathrm{B-H\ terminal}}$), 2245 ($\delta_{\mathrm{BH_2}}$ overtone), 2022 ($\nu_{\mathrm{B-H\ bridging}}$), 1946, 1441, 1360, 1134 ($\delta_{\mathrm{BH_2}}$). Anal. Calcd for $C_{28}H_{57}BCuNP_2$: C, 61.81; H, 10.56; N, 2.57. Found: C, 61.60; H, 10.53; N, 2.55.

Synthesis of ($^{t\mathrm{Bu}}$PN$^{\mathrm{H}}$P)Cu(BH$_4$) (2c). This compound was obtained as a white solid in 69% yield (0.50 mmol scale reaction) following a procedure similar to that used for **2a**. X-ray quality crystals were grown from a toluene/*n*-pentane solution. ^{1}H NMR (400 MHz, C_6D_6, δ): 2.70–2.56 (m, NCH_2, 4H), likely 1.75 (q, $J_{\mathrm{H-B}}$ = 85 Hz, BH_4, 4H), 1.50–1.38 (m, PCH_2, 4H), 1.36–1.07 (m, C(CH_3)$_3$, 36H); the NH resonance was not located. ^{13}C{^{1}H} NMR (101 MHz, C_6D_6, δ): 44.5 (s, NCH_2), 33.4 (t, $J_{\mathrm{C-P}}$ = 5.5 Hz, C(CH$_3$)$_3$), 29.7 (t, $J_{\mathrm{C-P}}$ = 3.8 Hz, C(CH$_3$)$_3$), 19.6 (t, $J_{\mathrm{C-P}}$ = 4.0 Hz, PCH_2). ^{31}P{^{1}H} NMR (162 MHz, C_6D_6, δ): 18.7 (s). ^{11}B NMR (128 MHz, C_6D_6, δ): −27.6 (quint, $J_{\mathrm{B-H}}$ = 82.3 Hz). Selected ATR-IR data (solid, cm^{-1}): 3299 ($\nu_{\mathrm{N-H}}$), 2937, 2895, 2863, 2795, 2353 ($\nu_{\mathrm{B-H\ terminal}}$), 2236 ($\delta_{\mathrm{BH_2}}$ overtone), 2058 ($\nu_{\mathrm{B-H\ bridging}}$), 1969, 1468, 1389, 1363, 1357, 1137 ($\delta_{\mathrm{BH_2}}$), 1128 ($\delta_{\mathrm{BH_2}}$). Anal. Calcd for $C_{20}H_{49}BCuNP_2$: C, 54.61; H, 11.23; N, 3.18. Found: C, 54.47; H, 11.23; N, 3.21.

Synthesis of ($^{i\mathrm{Pr}}$PN$^{\mathrm{Me}}$P)CuBr (4a). To an oven-dried Schlenk flask equipped with a stir bar were added $^{i\mathrm{Pr}}$PN$^{\mathrm{Me}}$P (479 mg, 1.50 mmol), CuBr (215 mg, 1.50 mmol), and 20 mL of THF. The resulting mixture was stirred for 16 h and then filtered through a plug of Celite to give a colorless solution, which was evaporated to dryness under vacuum. The residue was washed with *n*-pentane (10 mL × 3) and dried under vacuum to afford

the desired product as a white solid (590 mg, 85% yield). X-ray quality crystals were grown from a saturated CH_2Cl_2 solution layered with *n*-pentane and kept at −30 °C. ^{1}H NMR (400 MHz, C_6D_6, δ): 2.25 (s, NCH_3, 3H), 2.13–1.98 (m, 4H), 1.85–1.71 (m, 4H), 1.28–1.20 (m, 4H), 1.19–1.02 (m, CH(CH_3)$_2$, 24H). ^{13}C{^{1}H} NMR (101 MHz, C_6D_6, δ): 54.5 (t, J_{C-P} = 3.5 Hz, N*C*H$_3$), 44.3 (s, N*C*H$_2$), 24.2 (t, J_{C-P} = 7.5 Hz, *C*H(CH$_3$)$_2$), 22.2 (t, J_{C-P} = 6.4 Hz, P*C*H$_2$), 19.7 (t, J_{C-P} = 2.9 Hz, CH(*C*H$_3$)$_2$), 19.5 (t, J_{C-P} = 3.0 Hz, CH(*C*H$_3$)$_2$). ^{31}P{^{1}H} NMR (162 MHz, C_6D_6, δ): 2.7 (s). Selected ATR-IR data (solid, cm^{-1}): 2953, 2927, 2869, 2822, 2802, 1459, 1238, 1047. Anal. Calcd for $C_{17}H_{39}BrCuNP_2$: C, 44.11; H, 8.49; N, 3.03. Found: C, 43.86; H, 8.36; N, 3.07.

Representative procedure for catalytic hydrogenation of aldehydes and ketones

In a glovebox, an oven-dried Fischer–Porter tube equipped with a stir bar was charged with **1a** (9.0 mg, 0.020 mmol), KO^{t}Bu (0.020 mmol, from a 0.089 M stock solution in THF), and THF to reach a total volume of 3 mL. To the resulting mixture was added 1.0 mmol of the substrate. The sealed tube was taken outside the glovebox and flushed with H_2 three times, after which the H_2 pressure was set to an appropriate value based on the reactivity of the substrate. The reaction was stirred at room temperature for a desired period of time, and then H_2 was vented slowly. An aliquot of the reaction mixture was evaporated and dissolved in $CDCl_3$ for NMR analysis. The conversion of the substrate was calculated based on the ^{1}H NMR integrations. Selected alcohol products were subjected to purification on a pipette column packed with silica gel (eluted with a 4 : 1 mixture of EtOAc–hexanes).

Representative procedure for the reaction between 3a and a carbonyl substrate

To a dry J. Young NMR tube were added **3a** (3.3 mg, 2.5 μmol), a carbonyl substrate (25 μmol), and ~0.3 mL of C_6D_6. The progress of the reaction (at 23 °C) was periodically monitored by ^{1}H and ^{31}P{^{1}H} NMR spectroscopy.

Synthesis of (^{iPr}PN^{H}P)Cu(C_4H_3NCHO) (5a) from pyrrole-2-carboxaldehyde

To an oven-dried Schlenk flask equipped with a stir bar were added **1a** (90 mg, 0.20 mmol), KO^{t}Bu (27 mg, 0.24 mmol), and 10 mL of THF. The resulting mixture was stirred for 2 min, after which pyrrole-2-carboxaldehyde (19 mg, 0.20 mmol) was added. The reaction was kept at room temperature under stirring for 2 h, resulting in a color change from light yellow to orange. The volatiles were removed under vacuum and the residue was extracted with toluene (5 mL × 3). The combined toluene solutions were concentrated under vacuum, affording the product as an orange-yellow oil (68 mg, 73% yield). Attempts to crystallize the product from *n*-pentane were unsuccessful. ^{1}H NMR (400 MHz, C_6D_6, δ): 9.57 (s, C*H*O, 1 H), 7.48 (s, pyrrole C*H*, 1H), 7.22 (s, pyrrole C*H*, 1H), 6.62 (s, pyrrole C*H*, 1H), 4.12 (br, N*H*, 1H), 2.66–2.43 (m, 4H), 1.62–1.51 (m, 4H), 1.27–1.29 (m, 4H), 0.95–0.84 (m, CH(CH_3)$_2$, 24H). ^{13}C{^{1}H} NMR (101 MHz, C_6D_6, δ): 179.3 (s, *C*HO), 142.5 (s, pyrrole *C*), 140.3 (s, pyrrole *C*), 125.2 (s, pyrrole *C*), 111.9 (s, pyrrole *C*), 45.2 (s, N*C*H$_2$), 24.2 (t, J_{C-P} = 6.6 Hz, *C*H(CH$_3$)$_2$), 23.2 (t, J_{C-P} = 6.3 Hz, P*C*H$_2$), 19.2 (br, CH(*C*H$_3$)$_2$), 19.0 (br, CH(*C*H$_3$)$_2$). ^{31}P{^{1}H} NMR (162 MHz, C_6D_6, δ): 3.1 (s). Selected ATR-IR data (neat, cm^{-1}): 3243 (ν_{N-H}), 2952, 2927, 2868, 2754, 2717, 1622 ($\nu_{C=O}$), 1592, 1461, 1441, 1385, 1364, 1340, 1317. ESI-MS of **5a** in acetonitrile (*m*/*z*): [(^{iPr}PN^{H}P)Cu]$^+$ calcd for $C_{16}H_{37}NP_2Cu$ 368.16918, found 368.16908; [(^{iPr}PN^{H}P)Cu + O]$^+$ calcd for $C_{16}H_{37}NOP_2Cu$ 384.16409, found 384.16413; the parent ion of **5a** was not found.

X-ray structure determinations

Crystal data collection and refinement parameters are provided in the ESI.† Intensity data were collected at 150 K on a Bruker APEX-II CCD diffractometer using Mo Kα radiation, λ = 0.71073 Å. The data frames were processed using the program SAINT. The data were corrected for decay, Lorentz, and polarization effects as well as absorption and beam corrections based on the multi-scan technique. The structures were solved by a combination of direct methods and the difference Fourier technique as implemented in the SHELX suite of programs and refined by full-matrix least-squares on F^2. Non-hydrogen atoms were refined with anisotropic displacement parameters. For **2a** and **2c**, hydrogen atoms bound to N and B were located directly from the difference map; the coordinates were refined with the exception of the B-bound hydrogen atoms in **2c**. The B–H hydrogens for **2c** were held fixed at the located positions during the final stage of refinement. All remaining hydrogen atoms were calculated and treated with a riding model. Crystal structures mentioned in this paper have been deposited at the Cambridge Crystallographic Data Centre (CCDC) and allocated the deposition numbers CCDC 2089300–2089302.†

Conflicts of interest

There are no conflicts to declare.

Acknowledgements

We thank the NSF Chemical Catalysis Program (CHE-1464734 and CHE-1800151), the NSF MRI Program (CHE-0215950 for a Bruker APEX-II CCD diffractometer and CHE-1726092 for a Bruker Avance NEO 400 MHz NMR spectrometer), and the University of Cincinnati (Doctoral Enhancement Fellowship to D. A. Ekanayake and A. Chakraborty) for support of this research.

Notes and references

1 (*a*) S. Chakraborty and H. Guan, First-Row Transition Metal Catalyzed Reduction of Carbonyl Functionalities: A Mechanistic Perspective, *Dalton Trans.*, 2010, **39**, 7427–7436; (*b*) S. Chakraborty, P. Bhattacharya, H. Dai and H. Guan, Nickel and Iron Pincer Complexes as Catalysts for

the Reduction of Carbonyl Compounds, *Acc. Chem. Res.*, 2015, **48**, 1995–2003; (*c*) R. J. Trovitch, The Emergence of Manganese-Based Carbonyl Hydrosilylation Catalysts, *Acc. Chem. Res.*, 2017, **50**, 2842–2852; (*d*) S. R. Tamang and M. Findlater, Emergence and Applications of Base Metals (Fe, Co, and Ni) in Hydroboration and Hydrosilylation, *Molecules*, 2019, **24**, 3194; (*e*) Á. Raya-Barón, P. Oña-Burgos and I. Fernández, Iron-Catalyzed Homogeneous Hydrosilylation of Ketones and Aldehydes: Advances and Mechanistic Perspective, *ACS Catal.*, 2019, **9**, 5400–5417.

2 (*a*) W. H. Bernskoetter and N. Hazari, Hydrogenation and Dehydrogenation Reactions Catalyzed by Iron Pincer Compounds, in *Pincer Compounds: Chemistry and Applications*, ed. D. Morales-Morales, Elsevier, Amsterdam, 2018, ch. 6, pp. 111–131; (*b*) W. D. Jones, Hydrogenation/Dehydrogenation of Unsaturated Bonds with Iron Pincer Catalysis, *Top. Organomet. Chem.*, 2019, **63**, 141–174; (*c*) Z. Wei and H. Jiao, Bifunctional Aliphatic PNP Pincer Catalysts for Hydrogenation: Mechanisms and Scope, *Adv. Inorg. Chem.*, 2019, **73**, 323–384; (*d*) L. Alig, M. Fritz and S. Schneider, First-Row Transition Metal (De)Hydrogenation Catalysis Based on Functional Pincer Ligands, *Chem. Rev.*, 2019, **119**, 2681–2751; (*e*) D. A. Ekanayake and H. Guan, Hydrogenation Reactions Catalyzed by PNP-Type Complexes Featuring a HN $(CH_2CH_2PR_2)_2$ Ligand, *Top. Organomet. Chem.*, 2021, **68**, 263–320.

3 (*a*) P. A. Dub, N. J. Henson, R. L. Martin and J. C. Gordon, Unravelling the Mechanism of the Asymmetric Hydrogenation of Acetophenone by $[RuX_2$(diphosphine)(1,2-diamine)] Catalysts, *J. Am. Chem. Soc.*, 2014, **136**, 3505–3521; (*b*) P. A. Dub and J. C. Gordon, Metal–Ligand Bifunctional Catalysis: The "Accepted" Mechanism, the Issue of Concertedness, and the Function of the Ligand in Catalytic Cycles Involving Hydrogen Atoms, *ACS Catal.*, 2017, **7**, 6635–6655; (*c*) P. A. Dub and J. C. Gordon, The Role of the Metal-Bound N–H Functionality in Noyori-Type Molecular Catalysts, *Nat. Rev. Chem.*, 2018, **2**, 396–408.

4 K. V. Vasudevan, B. L. Scott and S. K. Hanson, Alkene Hydrogenation Catalyzed by Nickel Hydride Complexes of an Aliphatic PNP Pincer Ligand, *Eur. J. Inorg. Chem.*, 2012, 4898–4906.

5 (*a*) W. S. Mahoney, D. M. Brestensky and J. M. Stryker, Selective Hydride-Mediated Conjugate Reduction of α,β-Unsaturated Carbonyl Compounds Using $[(Ph_3P)CuH]_6$, *J. Am. Chem. Soc.*, 1988, **110**, 291–293; (*b*) W. S. Mahoney and J. M. Stryker, Hydride-Mediated Homogeneous Catalysis. Catalytic Reduction of α,β-Unsaturated Ketones Using $[(Ph_3P)CuH]_6$ and H_2, *J. Am. Chem. Soc.*, 1989, **111**, 8818–8823.

6 (*a*) J.-X. Chen, J. F. Daeuble, D. M. Brestensky and J. M. Stryker, Highly Chemoselective Catalytic Hydrogenation of Unsaturated Ketones and Aldehydes to Unsaturated Alcohols Using Phosphine-Stabilized Copper (I) Hydride Complexes, *Tetrahedron*, 2000, **56**, 2153–2166; (*b*) J.-X. Chen, J. F. Daeuble and J. M. Stryker, Phosphine Effects in the Copper(I) Hydride-Catalyzed Hydrogenation of Ketones and Regioselective 1,2-Reduction of α,β-Unsaturated Ketones and Aldehydes. Hydrogenation of Decalin and Steroidal Ketones and Enones, *Tetrahedron*, 2000, **56**, 2789–2798.

7 T. Nakajima, K. Nakamae, Y. Ura and T. Tanase, Multinuclear Copper Hydride Complexes Supported by Polyphosphine Ligands, *Eur. J. Inorg. Chem.*, 2020, 2211–2226.

8 C. M. Zall, J. C. Linehan and A. M. Appel, Triphosphine-Ligated Copper Hydrides for CO_2 Hydrogenation: Structure, Reactivity, and Thermodynamic Studies, *J. Am. Chem. Soc.*, 2016, **138**, 9968–9977.

9 C. M. Zall, J. C. Linehan and A. M. Appel, A Molecular Copper Catalyst for Hydrogenation of CO_2 to Formate, *ACS Catal.*, 2015, **5**, 5301–5305.

10 K. Nakamae, T. Nakajima, Y. Ura, Y. Kitagawa and T. Tanase, Facially Dispersed Polyhydride Cu_9 and Cu_{16} Clusters Comprising Apex-Truncated Supertetrahedral and Square-Face-Capped Cuboctahedral Copper Frameworks, *Angew. Chem., Int. Ed.*, 2020, **59**, 2262–2267.

11 (*a*) H. Shimizu, D. Igarashi, W. Kuriyama, Y. Yusa, N. Sayo and T. Saito, Asymmetric Hydrogenation of Aryl Ketones Mediated by a Copper Catalyst, *Org. Lett.*, 2007, **9**, 1655–1657; (*b*) H. Shimizu, T. Nagano, N. Sayo, T. Saito, T. Ohshima and K. Mashima, Asymmetric Hydrogenation of Heteroaromatic Ketones and Cyclic and Acyclic Enones Mediated by Cu(I)-Chiral Diphosphine Catalysts, *Synlett*, 2009, 3143–3146; (*c*) S. W. Krabbe, M. A. Hatcher, R. K. Bowman, M. B. Mitchell, M. S. McClure and J. S. Johnson, Copper-Catalyzed Asymmetric Hydrogenation of Aryl and Heteroaryl Ketones, *Org. Lett.*, 2013, **15**, 4560–4563; (*d*) O. V. Zatolochnaya, S. Rodríguez, Y. Zhang, K. S. Lao, S. Tcyrulnikov, G. Li, X.-J. Wang, B. Qu, S. Biswas, H. P. R. Mangunuru, D. Rivalti, J. D. Sieber, J.-N. Desrosiers, J. C. Leung, N. Grinberg, H. Lee, N. Haddad, N. K. Yee, J. J. Song, M. C. Kozlowski and C. H. Senanayake, Copper-Catalyzed Asymmetric Hydrogenation of 2-Substituted Ketones *via* Dynamic Kinetic Resolution, *Chem. Sci.*, 2018, **9**, 4505–4510; (*e*) K. Junge, B. Wendt, D. Addis, S. Zhou, S. Das, S. Fleischer and M. Beller, Copper-Catalyzed Enantioselective Hydrogenation of Ketones, *Chem. – Eur. J.*, 2011, **17**, 101–105.

12 H. Shimizu, N. Sayo and T. Saito, A Practical and Highly Chemoselective Hydrogenation of Aldehydes with a Copper Catalyst, *Synlett*, 2009, 1295–1298.

13 R. Watari, Y. Kayaki, S. Hirano, N. Matsumoto and T. Ikariya, Hydrogenation of Carbon Dioxide to Formate Catalyzed by a Copper/1,8-Diazabicyclo[5.4.0]undec-7-ene System, *Adv. Synth. Catal.*, 2015, **357**, 1369–1373.

14 H. Liu, Q. Mei, Q. Xu, J. Song, H. Liu and B. Han, Synthesis of Formamides Containing Unsaturated Groups by *N*-Formylation of Amines Using CO_2 with H_2, *Green Chem.*, 2017, **19**, 196–201.

15 K. Chaudhary, M. Trivedi, D. T. Masram, A. Kumar, G. Kumar, A. Husain and N. P. Rath, A Highly Active

Copper Catalyst for the Hydrogenation of Carbon Dioxide to Formate under Ambient Conditions, *Dalton Trans.*, 2020, **49**, 2994–3000.

16 (*a*) C. Deutsch, N. Krause and B. H. Lipshutz, CuH-Catalyzed Reactions, *Chem. Rev.*, 2008, **108**, 2916–2927; (*b*) A. J. Jordan, G. Lalic and J. P. Sadighi, Coinage Metal Hydrides: Synthesis, Characterization, and Reactivity, *Chem. Rev.*, 2016, **116**, 8318–8372.

17 S. S. Rozenel, J. B. Kerr and J. Arnold, Metal Complexes of Co, Ni and Cu with the Pincer Ligand $HN(CH_2CH_2P^iPr_2)_2$: Preparation, Characterization and Electrochemistry, *Dalton Trans.*, 2011, **40**, 10397–10405.

18 D. A. Ekanayake, A. Chakraborty, J. A. Krause and H. Guan, Steric Effects of $HN(CH_2CH_2PR_2)_2$ on the Nuclearity of Copper Hydrides, *Inorg. Chem.*, 2020, **59**, 12817–12828.

19 (*a*) S. Chakraborty, J. Zhang, Y. J. Patel, J. A. Krause and H. Guan, Pincer-Ligated Nickel Hydridoborate Complexes: the Dormant Species in Catalytic Reduction of Carbon Dioxide with Borane, *Inorg. Chem.*, 2013, **52**, 37–47; (*b*) S. Qu, H. Dai, Y. Dang, C. Song, Z.-X. Wang and H. Guan, Computational Mechanistic Study of Fe-Catalyzed Hydrogenation of Esters to Alcohols: Improving Catalysis by Accelerating Precatalyst Activation with a Lewis Base, *ACS Catal.*, 2014, **4**, 4377–4388; (*c*) S. Murugesan, B. Stöger, M. Weil, L. F. Verios and K. Kirchner, Synthesis, Structure, and Reactivity of Co(II) and Ni(II) PCP Pincer Borohydride Complexes, *Organometallics*, 2015, **34**, 1364–1372.

20 (*a*) T. Ohkuma, M. Koizumi, K. Muñiz, G. Hilt, C. Kabuto and R. Noyori, *trans*-RuH(η^1-BH_4)(binap)(1,2-diamine): A Catalyst for Asymmetric Hydrogenation of Simple Ketones under Base-Free Conditions, *J. Am. Chem. Soc.*, 2002, **124**, 6508–6509; (*b*) R. Guo, X. Chen, C. Elpelt, D. Song and R. H. Morris, Applications of Ruthenium Hydride Borohydride Complexes Containing Phosphinite and Diamine Ligands to Asymmetric Catalytic Reactions, *Org. Lett.*, 2005, **7**, 1757–1759.

21 (*a*) W. Kuriyama, T. Matsumoto, O. Ogata, Y. Ino, K. Aoki, S. Tanaka, K. Ishida, T. Kobayashi, N. Sayo and T. Saito, Catalytic Hydrogenation of Esters. Development of an Efficient Catalyst and Processes for Synthesising (*R*)-1,2-Propanediol and 2-(*l*-Menthoxy)ethanol, *Org. Process Res. Dev.*, 2012, **16**, 166–171; (*b*) Z. Han, L. Rong, J. Wu, L. Zhang, Z. Wang and K. Ding, Catalytic Hydrogenation of Cyclic Carbonates: A Practical Approach from CO_2 and Epoxides to Methanol and Diols, *Angew. Chem., Int. Ed.*, 2012, **51**, 13041–13045.

22 (*a*) S. Chakraborty, H. Dai, P. Bhattacharya, N. T. Fairweather, M. S. Gibson, J. A. Krause and H. Guan, Iron-Based Catalysts for the Hydrogenation of Esters to Alcohols, *J. Am. Chem. Soc.*, 2014, **136**, 7869–7872; (*b*) S. Werkmeister, K. Junge, B. Wendt, E. Alberico, H. Jiao, W. Baumann, H. Jung, F. Gallou and M. Beller, Hydrogenation of Esters to Alcohols with a Well-Defined Iron Complex, *Angew. Chem., Int. Ed.*, 2014, **53**, 8722–8726; (*c*) S. Elangovan, B. Wendt, C. Topf, S. Bachmann, M. Scalone, A. Spannenberg, H. Jiao, W. Baumann, K. Jung and M. Beller, Improved Second Generation Iron Pincer Complexes for Effective Ester Hydrogenation, *Adv. Synth. Catal.*, 2016, **358**, 820–825; (*d*) F. Schneck, M. Assmann, M. Balmer, K. Harms and R. Langer, Selective Hydrogenation of Amides to Amines and Alcohols Catalyzed by Improved Iron Pincer Complexes, *Organometallics*, 2016, **35**, 1931–1943; (*e*) N. M. Rezayee, D. C. Samblanet and M. S. Sanford, Iron-Catalyzed Hydrogenation of Amides to Alcohols and Amines, *ACS Catal.*, 2016, **6**, 6377–6383; (*f*) M. Garbe, Z. Wei, B. Tannert, A. Spannenberg, H. Jiao, S. Bachmann, M. Scalone, K. Junge and M. Beller, Enantioselective Hydrogenation of Ketones Using Different Metal Complexes with a Chiral PNP Pincer Ligand, *Adv. Synth. Catal.*, 2019, **361**, 1913–1920; (*g*) H. Dai, W. Li, J. A. Krause and H. Guan, Experimental Evidence of *syn* H–N–Fe–H Configurational Requirement for Iron-Based Bifunctional Hydrogenation Catalysts, *Inorg. Chem.*, 2021, **60**, 6521–6535.

23 J. B. Curely, N. E. Smith, W. H. Bernskoetter, N. Hazari and B. Q. Mercado, Catalytic Formic Acid Dehydrogenation and CO_2 Hydrogenation Using Iron PN^RP Pincer Complexes with Isonitrile Ligands, *Organometallics*, 2018, **37**, 3846–3853.

24 (*a*) S. J. Lippard and K. M. Melmed, Transition Metal Borohydride Complexes. I. The Structure of Borohydridobis (triphenylphosphine)copper(I), *J. Am. Chem. Soc.*, 1967, **89**, 3929–3930; (*b*) S. J. Lippard and D. A. Ucko, Transition Metal Borohydride Complexes. II. The Reaction of Copper (I) Compounds with Boron Hydride Anions, *Inorg. Chem.*, 1968, **7**, 1051–1056; (*c*) B. E. Green, C. H. L. Kennard, G. Smith, M. M. Elcombe, F. H. Moore, B. D. James and A. H. White, Crystal Structures of α- and β-(1,10-Phenanthroline)tetrahydroborato(triphenylphosphine) copper(I) and (2,9-Dimethyl-4,7-diphenyl-1,10-phenanthroline)tetrahydroboratocopper(I), *Inorg. Chim. Acta*, 1984, **83**, 177–189; (*d*) M. Lueckheide, N. Rothman, B. Ko and J. M. Tanski, π-Stacking Motifs in the Crystal Structures of Bis(phosphine) Copper(I) η^2-Tetrahydroborate Complexes, *Polyhedron*, 2013, **58**, 79–84; (*e*) X. Hu, M. Soleihavoup, M. Melaimi, J. Chu and G. Bertrand, Air-Stable (CAAC)CuCl and (CAAC)$CuBH_4$ Complexes as Catalysts for the Hydrolytic Dehydrogenation of BH_3NH_3, *Angew. Chem., Int. Ed.*, 2015, **54**, 6008–6011; (*f*) N. V. Belkova, I. E. Golub, E. I. Gutsul, K. A. Lyssenko, A. S. Peregudov, V. D. Makhaev, O. A. Filippov, L. M. Epstein, A. Rossin, M. Peruzzini and E. S. Shubina, Binuclear Copper(I) Borohydride Complex Containing Bridging Bis(diphenylphosphino) Methane Ligands: Polymorphic Structures of $[(\mu_2\text{-dppm})_2Cu_2(\eta^2\text{-}BH_4)_2]$ Dichloromethane Solvate, *Crystals*, 2017, **7**, 318.

25 G. F. Svatos, C. Curran and J. V. Quagliano, Infrared Absorption Spectra of Inorganic Coordination Complexes. V. The N–H Stretching Vibration in Coordination Compounds, *J. Am. Chem. Soc.*, 1955, **77**, 6159–6163.

26 J. Joseph and E. D. Jemmis, Red-, Blue-, or No-Shift in Hydrogen Bonds: A Unified Explanation, *J. Am. Chem. Soc.*, 2007, **129**, 4620–4632.

27 T. Seki, T. Nakajo and M. Onaka, The Tishchenko Reaction: A Classic and Practical Tool for Ester Synthesis, *Chem. Lett.*, 2006, **35**, 824–829.

28 W. D. Phillips, H. C. Miller and E. L. Muetterties, B^{11} Magnetic Resonance Study of Boron Compounds, *J. Am. Chem. Soc.*, 1959, **81**, 4496–4500.

29 (*a*) T. H. Lemmen, K. Folting, J. C. Huffman and K. G. Caulton, Copper Polyhydrides, *J. Am. Chem. Soc.*, 1985, **107**, 7774–7775; (*b*) D. M. Brestensky, D. E. Huseland, C. McGettigan and J. M. Stryker, Simplified, "One-Pot" Procedure for the Synthesis of $[(Ph_3P)CuH]_6$, a Stable Copper Hydride for Conjugate Reductions, *Tetrahedron Lett.*, 1988, **29**, 3749–3752.

30 K. Azizi and R. Madsen, Radical Condensation Between Benzylic Alcohols and Acetamides to Form 3-Arylpropanamides, *Chem. Sci.*, 2020, **11**, 7800–7806.

31 N. A. Eberhardt, N. P. N. Wellala, Y. Li, J. A. Krause and H. Guan, Dehydrogenative Coupling of Aldehydes with Alcohols Catalyzed by a Nickel Hydride Complex, *Organometallics*, 2019, **38**, 1468–1478.

32 (*a*) Y. Watanabe, K. Sawada and M. Hayashi, A Green Method for the Self-Aldol Condensation of Aldehydes Using Lysine, *Green Chem.*, 2010, **12**, 384–386; (*b*) L. K. Sharma, K. B. Kim and G. I. Elliott, A Selective Solvent-Free Self-Condensation of Carbonyl Compounds Utilizing Microwave Irradiation, *Green Chem.*, 2011, **13**, 1546–1549.

33 Both GC-MS and NMR could confirm the allylic alcohol product; however, a number of other unidentified products were also present, possibly resulting from various enolate addition reactions. Compared to the Stryker's catalyst, the $^{R}PN^{H}P$-ligated copper system reported here may be more basic, promoting enolate chemistry.

34 (*a*) D. M. L. Goodgame and F. A. Cotton, Phosphine Oxide Complexes. Part IV. Tetrahedral, Planar, and Binuclear Complexes of Copper(II) with Phosphine Oxides, and Some Arsine Oxide Analogues, *J. Chem. Soc.*, 1961, 2298–2305; (*b*) G. Pilloni, G. Valle, C. Corvaja, B. Longato and B. Corain, Copper(II) and Copper(I) Complexes Stabilized by Phosphine Oxides: Synthesis and Characterization of the Cationic Complexes $[Cu(odppf)_2(EtOH)]^{2+}$ and $[Cu(odppf)_2]^{2+}$, Precursors of the Novel Copper(I) Adduct $[Cu(odppf)_2]^{+}$ (odppf = 1,1′-Bis(oxodiphenylphosphoranyl) ferrocene). Crystal Structure of $[Cu(odppf)_2(EtOH)](BF_4)_2$ and $[Cu(odppf)_2](BF_4)_2$, *Inorg. Chem.*, 1995, **34**, 5910–5918.

35 Though we do not have evidence supporting that $(^{iPr}PN^{H}P)_nCu_nH_n$ (n = 1–3) exist, structures of (κ^2-triphos)$_2Cu_2H_2$, [(*S*)-SEGPHOS]$_2Cu_2H_2$ ((*S*)-SEGPHOS is a chiral diphosphine), and (dppbz)$_3Cu_3H_3$ (dppbz = 1,2-bis (diphenylphosphino)benzene) have been reported. For details, see: (*a*) G. V. Goeden, J. C. Huffman and K. G. Caulton, A Cu–(μ-H) Bond Can Be Stronger Than an Intramolecular P→Cu Bond. Synthesis and Structure of $Cu_2(\mu\text{-}H)_2[\eta^2\text{-}CH_3C(CH_2PPh_2)_3]_2$, *Inorg. Chem.*, 1986, **25**, 2484–2485; (*b*) Y. Xi and J. F. Hartwig, Mechanistic Studies of Copper-Catalyzed Asymmetric Hydroboration of Alkenes, *J. Am. Chem. Soc.*, 2017, **139**, 12758–12772; (*c*) M. S. Eberhart, J. R. Norton, A. Zuzek, W. Sattler and S. Ruccolo, Electron Transfer from Hexameric Copper Hydrides, *J. Am. Chem. Soc.*, 2013, **135**, 17262–17265.

36 N. P. Fitzsimons, W. Jones and P. J. Herley, Studies of Copper Hydride. Part 1. – Synthesis and Solid-State Stability, *J. Chem. Soc., Faraday Trans.*, 1995, **91**, 713–718.

37 P. A. Dub, B. L. Scott and J. C. Gordon, Why Does Alkylation of the N–H Functionality within M/NH Bifunctional Noyori-Type Catalysts Lead to Turnover?, *J. Am. Chem. Soc.*, 2017, **139**, 1245–1260.

38 (*a*) Y. Zhang, A. D. MacIntosh, J. L. Wong, E. A. Bielinski, P. G. Williard, B. Q. Mercado, N. Hazari and W. H. Bernskoetter, Iron Catalyzed CO_2 Hydrogenation to Formate Enhanced by Lewis Acid Co-Catalysts, *Chem. Sci.*, 2015, **6**, 4291–4299; (*b*) J. Yuwen, S. Chakraborty, W. W. Brennessel and W. D. Jones, Additive-Free Cobalt-Catalyzed Hydrogenation of Esters to Alcohols, *ACS Catal.*, 2017, **7**, 3735–3740; (*c*) U. Jayarathne, N. Hazari and W. H. Bernskoetter, Selective Iron-Catalyzed *N*-Formylation of Amines Using Dihydrogen and Carbon Dioxide, *ACS Catal.*, 2018, **8**, 1338–1345.

39 Because nitrogen and phosphorus are separated by two carbon atoms, the electronic and steric effects of NH *vs.* N-alkyl on the phosphorus donor ability should be similar.

40 L. Yang, D. R. Powell and R. P. Houser, Structural Variation in Copper(I) Complexes with Pyridylmethylamide Ligands: Structural Analysis with a New Four-Coordinate Geometry Index, τ_4, *Dalton Trans.*, 2007, 955–964.

41 T-shaped Cu(I) complexes supported a PNP pincer ligand are known in the literature, although the central donor is pyridine-based. For examples, see: (*a*) J. I. van der Vlugt, E. A. Pidko, D. Vogt, M. Lutz, A. L. Spek and A. Meetsma, T-Shaped Cationic Cu^{I} Complexes with Hemilabile PNP-Type Ligands, *Inorg. Chem.*, 2008, **47**, 4442–4444; (*b*) J. I. van der Vlugt, E. A. Pidko, D. Vogt, M. Lutz and A. L. Spek, Cu^{I} Complexes with a Noninnocent PNP Ligand: Selective Dearomatization and Electrophilic Addition Reactivity, *Inorg. Chem.*, 2009, **48**, 7513–7515; (*c*) K. Takeuchi, Y. Tanaka, I. Tanigawa, F. Ozawa and J.-C. Choi, Cu(I) Complex Bearing a PNP-Pincer-Type Phosphaalkene Ligand with a Bulky Fused-Ring Eind Group: Properties and Applications to FLP-Type Bond Activation and Catalytic CO_2 Reduction, *Dalton Trans.*, 2020, **49**, 3630–3637.

42 G. V. Goeden and K. G. Caulton, Soluble Copper Hydrides: Solution Behavior and Reactions Related to CO Hydrogenation, *J. Am. Chem. Soc.*, 1981, **103**, 7354–7355.

43 O. G. Shirobokov, L. G. Kuzmina and G. I. Nikonov, Nonhydride Mechanism of Metal-Catalyzed Hydrosilylation, *J. Am. Chem. Soc.*, 2011, **133**, 6487–6489.

44 B. L. Tran, B. D. Neisen, A. L. Speelman, T. Gunasekara, E. S. Wiedner and R. M. Bullock, Mechanistic Studies on the Insertion of Carbonyl Substrates into Cu-H: Different Rate-Limiting Steps as a Functional of Electrophilicity, *Angew. Chem., Int. Ed.*, 2020, **59**, 8645–8653.

45 G. Xu, S. Leloux, P. Zhang, J. Meijide Suárez, Y. Zhang, E. Derat, M. Ménand, O. Bistri-Aslanoff, S. Roland, T. Leyssens, O. Riant and M. Sollogoub, Capturing the Monomeric (L)CuH in NHC-Capped Cyclodextrin: Cavity-Controlled Chemoselective Hydrosilylation of α,β-Unsaturated Ketones, *Angew. Chem., Int. Ed.*, 2020, **59**, 7591–7597.

46 The chemical shift value for the NH resonance (4.12 ppm) and the broadening of the NH stretching band suggest some weak HBI between the NH group and the oxygen atom of the carbonyl group. For a reference to varying degrees of HBIs in $^{iPr}PN^{H}P$-ligated metal complexes, see: N. P. N. Wellala, J. D. Luebking, J. A. Krause and H. Guan, Roles of Hydrogen Bonding in Proton Transfer to $\kappa^{P},\kappa^{P},\kappa^{P}$-N$(CH_2CH_2P^{i}Pr_2)_2$-Ligated Nickel Pincer Complexes, *ACS Omega*, 2018, **3**, 4986–5001.

47 We also examined the reduction of 4-(trifluoromethyl)benzaldehyde, *o*-tolualdehyde, and 2-fluorobenzaldehyde with **3a**, which all yielded the expected insertion products.

48 G. M. Whitesides, J. S. Sadowski and J. Lilburn, Copper(I) Alkoxides. Synthesis, Reactions, and Thermal Decomposition, *J. Am. Chem. Soc.*, 1974, **96**, 2829–2835.

49 We cannot rule out the possibility that the carbonyl insertion step takes place on $(^{R}PN^{H}P)_nCu_nH_n$ or $(^{R}PN^{H}P)_nCu_{2n}H_{2n}$ (n = 2, 3) whereas regeneration of the hydride from the copper alkoxide intermediate involves a mononuclear species with NH coordination. If this holds true, a significant NH effect could also be observed.

50 In principle, the hydrogenolysis and cooperative elimination mechanisms can be differentiated by tracking deuterium during a stoichiometric reaction between ($^{iPr}PN^{D}P$)CuH (generated from ($^{iPr}PN^{D}P$)CuBr or ($^{iPr}PN^{D}P)_3Cu_6H_6$) and a carbonyl substrate. Such an effort was discouraged by the fact that ($^{iPr}PN^{H}P$)CuBr and ($^{iPr}PN^{H}P)_3Cu_6H_6$ undergo rapid H/D exchange between the NH hydrogen and deuterated alcohols (CD_3OD or ^{t}BuOD).

51 The solution color during ketone hydrogenation (catalyzed by **1a**-KO^{t}Bu) is noticeably darker than the color observed during aldehyde hydrogenation, hinting that a higher percentage of the copper hydride is in the cluster form.

52 S. Werkmeister, K. Junge, B. Wendt, E. Alberico, H. Jiao, W. Baumann, H. Jung, F. Gallou and M. Beller, Hydrogenation of Esters to Alcohols with a Well-Defined Iron Complex, *Angew. Chem., Int. Ed.*, 2014, **53**, 8722–8726.